PRECISION FREQUENCY CONTROL

OF A MAGNETIC STORAGE DRUM

by

Hermann Josef Fink

B.A.Sc., University of British Columbia, 1955

A thesis submitted in partial fulfilment of

the requirements for the degree of

Master of Applied Science

in the department of

Electrical Engineering

We accept this thesis as conforming to

the standard required from candidates for

the degree of Master of Applied Science.

Members of the Department

of Electrical Engineering

The University of British Columbia

October, 1956

In presenting this thesis in partial fulfilment of the requirements for an advanced degree at the University of British Columbia, I agree that the Library shall make it freely available for reference and study. I further agree that permission for extensive copying of this thesis for scholarly purposes may be granted by the Head of my Department or by his representative. It is understood that copying or publication of this thesis for financial gain shall not be allowed without my written permission.

Department of ELECTRICAL ENGINEERING

The University of British Columbia,
Vancouver 8, Canada.

Date OCTOBER 10, 1956

ABSTRACT

In the development of a pulse position modulation analogue computer the requirement arose to control accurately the frequency of a magnetic drum. A control system was designed which compares the drum frequency to a 1000 cps tuning fork oscillator. Any deviation in phase produces a corresponding change in torque on the drum drive motor which then corrects the phase error.

As part of the over-all project a precision power supply was developed. The requirements were met by modifying existing designs.

List of Contents

		Page
Chapter I	Introduction	1
	Drum Control System	2
	System Requirements	3
Chapter II	The Servo Control System	5
	Evaluation of Drum Constants	13
	Servo Amplifier and Stabilizing Loop	18
	Phase Inverter and Push-Pull Amplifier	20
Chapter III	The Drum Synchronizer	21
	Amplifier and Peaker	23
	Phantastron Divider	23
	Phantastron Analysis	27
	Phase sensitive Detector and Motor Driving Stage	29
	Monostable Cathode Coupled Multivibrator	32
Chapter IV	Experimental Determination of the Describing Function $G(S,\emptyset_i)$	35
	Test of the Over-all System	43
Chapter V	Revised Design	44
Chapter VI	The Precision Power Supply	54
	Introduction	54
	General Description	54
	Calibration Procedure	61
	References	62
Appendix	List of Components	63

List of Figures

Figure		Page
1	Input Circuitry to the Drum Motor	6
2	(a) Simplified Block Diagram of Servo Loop	8
	(b) Transfer Function ϕ_M/ϕ_i	8
	(c) Asymptotic Plot of ϕ_M/ϕ_i	8
3	Current and Voltage Characteristics of Motor M_4	15
4	Servo Amplifier and Stabilizing Loop	19
5	Block Diagram of Drum Synchronizer	22
6	Amplifier and Peaker	24
7	(a) Phantastron Divider	26
	(b) Grid and Plate Voltages during the Sweep	26
8	Phase Sensitive Rectifier and Motor Driving Stage	30
9	Phase Shifter and Resolver Drivers	31
10	Monostable Cathode Coupled Multivibrator	33
11	Test Procedure for Measuring Gain Characteristics and Phase Shift of the Non-linear portion of the Servo System	36
12	Gain and Phase Characteristics of the Non-linear part of the Transfer Function	38
13	Gain and Phase Characteristics of Open Loop Transfer Function	39
14	Nyquist Diagram (General Shape)	40
15	Circuit Modifications due to Stability Considerations	42
16	Block Diagram of Revised Design	45
17	Phase Sensitive Rectifier, Lead Network, Amplifier and Balanced Modulator	48
18	Open and Closed Loop Response of Revised Design	49

19	Open and Closed Loop Response	50
20	60 cps Balanced Modulator, Power Amplifier, and Bias Setting of Drum Drive Motor	52
21	Precision Power Supply Between -300V DC and Ground, 450 mA	56
22	DC Comparison Circuit and Amplifier, George A. Philbrick, Model K2-R	57
23	Modulator Comparison Circuit	58
24	Precision Power Supply Between +300V DC and Ground, 450 mA	59
25	Modulator Comparison Circuit	60

ACKNOWLEDGEMENT

The work described in this thesis is part of a project sponsored by the Defence Research Board, Department of National Defence, Canada, under Grant Number DRB C-9931-02-(550-GC).

Acknowledgement is gratefully given to Dr. E. V. Bohn, under whose guidance this work was performed, to Dr. F. Noakes, grantee of the project, and to Dr. A. D. Moore, all of the Department of Electrical Engineering, The University of British Columbia.

The author is indebted to the British Columbia Electric Railway Company for a scholarship granted in 1955 and to the Defence Research Board, Department of National Defence, Canada, for the assistance received.

CHAPTER I

INTRODUCTION

In the development of a pulse position modulation analogue computer the requirement arose for accurate control of the frequency of a magnetic drum. This thesis concerns itself with the design of the entire control system to meet this requirement. In addition, as part of the over-all project, stable precision power supplies were developed with an output voltage of $\pm$ 300 volts DC, having both short term and long term stability.

DRUM CONTROL SYSTEM

The drum has a clock track containing 1560 notches filled with iron oxide. For the purpose of handling the information one track is divided up into 15 channels, each channel containing 104 pulses. To control the frequency of the drum a 1000 cps G.R. tuning fork oscillator is taken as a reference frequency standard, the repetition rate of a channel is taken as 1 milli-second. The frequency from the clock track is therefore 104 kcps. Two phantastron dividers are used to divide by 8 x 13. The output of the divider network is a 1000 cps square wave. The phase of the square wave is compared with that of the 1000 cps standard by means of a phase sensitive rectifier. The DC error output is used to control the torque of the drum drive motor which then corrects the phase error.

The storage drum is controlled by a series AC-DC motor. A stable loop must now be designed between the output of the phase sensitive rectifier and the drum drive motor. The steady state volt-ampere requirements of 30 VA make an all electronic control expensive. Therefore it was decided to use a variac control for the drive motor.

SYSTEM REQUIREMENTS

If the system is to function adequately it must be stable and must have a frequency lock on range which is not too narrow. If there is a frequency error the phase sensitive rectifier will give a fluctuating output and the system may not lock on. It is therefore desirable to have first a region of frequency control and then when the frequency error is sufficiently small, the system should lock on in phase. The inputs to the system are the random torque variation due to change in the line voltage, changes in mechanical friction and random phase drift of the tuning fork.[11] The servo system must have a rapid enough response to follow and compensate for these random variations. A constant voltage transformer of $\pm$ 1% regulation reduces voltage variations of the variac output. A phase lock of the drum may be provided within $\pm 90^\circ$ of the 1000 cps standard or within $\pm 90^\circ \div 15 = \pm 6^\circ$ of the reference point on the drum.

To estimate the minimum variac speed required to follow random phase variations refer to equation (4) chapter II.

For a step input $\phi_M = \frac{|\phi_M|}{S}$ we get $\beta = \frac{\left(e^{-\frac{t}{\tau_4}} + \frac{t}{\tau_4} - 1\right) \times 12.78 \times |\phi_M|}{\left(\frac{1}{\tau_4}\right)^2}$,

for smaller values of t we have

$$\beta = 12.78 \times |\phi_M| \frac{t^2}{2}.$$

We now assume the phase variation to be of the order of 24°/sec.

Then

$$\phi_M = \frac{2 \times 24}{12.78} = \pm 3.75^\circ.$$

The variac should be able to move at a rate of at least $\pm$ 3.75°/sec. This would probably ensure phase lock provided phase changes were notgreater than 24°/sec. Due to the large inertia of the drum this seems like a reasonable assumption.

The drum synchronizer discussed in Chapter III consists of the phantastron dividers, the phase sensitive rectifier and an electro-mechanical phase detector. (Fig. 5) The range of frequency lock on is determined mainly by the response of the motor M_1 and the gear ratio N_1. If the gear ratio N_1 is chosen large the servo will not be able to pull in for rapid phase variations and if N_1 is chosen small the smoothness of phase lock on will suffer. For continuous rotation of M_1 the tachometer will supply a driving voltage to turn the variac drive motor in the required direction. As soon as the frequency error has been reduced sufficiently, the tachometer voltage becomes smaller and the phase sensitive rectifier now operates to give zero phase error. The variac then undergoes a damped low frequency oscillation until phase lock is achieved.

CHAPTER II

THE SERVO CONTROL SYSTEM

Consider figure 1. An error voltage ϵ will produce a torque on the motor M_3 which will turn through an angle ϕ_M. This will cause a shift in the position of the variac and therefore increase or decrease the voltage input to the series motor which drives the drum. An increase in voltage will accelerate the drum, a decrease in voltage will decelerate the drum.

The drum has eleven tracks. One track is used to synchronize the operation of the computer. On this track one hundred lines per inch are etched around the whole circumference of the drum. They produce a signal whose waveform is approximately sinusoidal and which is 104 kcps when the drum is rotating with 4000 RPM. Any phase error of the drum will appear as a phase error β of the square wave signal. The phase error β is fed into the drum synchronizer,* the output of which is 15β.

* For details of drum synchronizer see Chapter III.

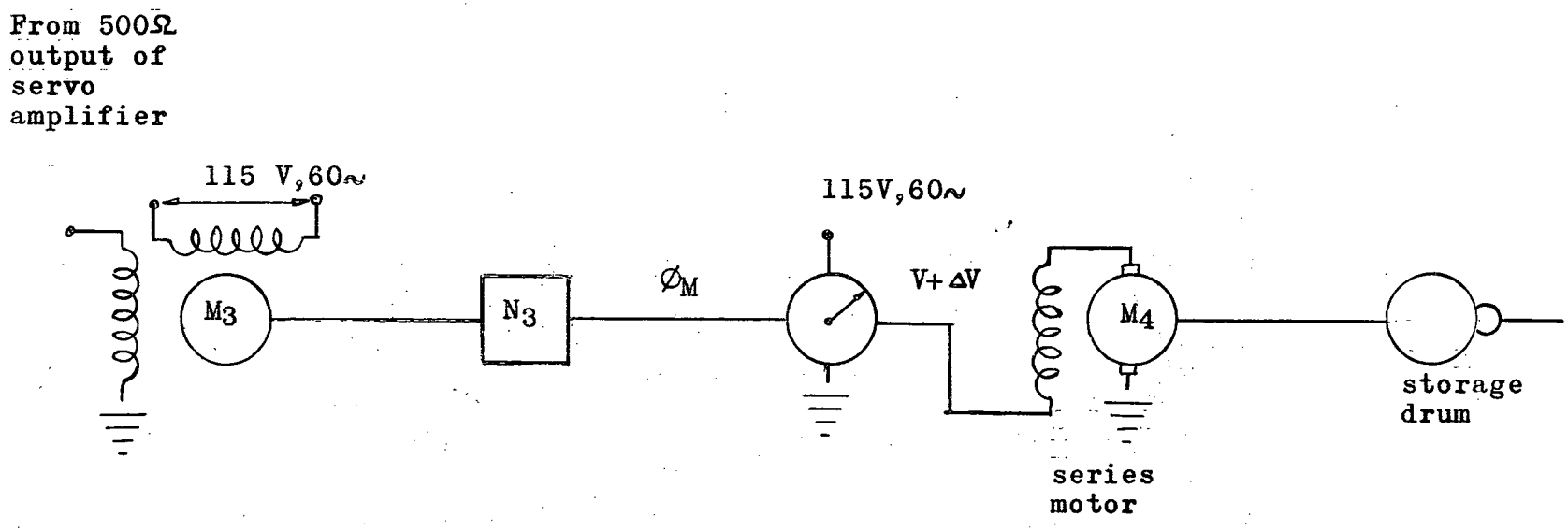

Figure 1. Input Circuitry to the Drum Motor

Consider Fig. 1. We see that the variac drive motor and the drum motor are in cascade. This would lead to a transfer function of the form

$$\frac{K}{S^2 \left(S + \frac{1}{\tau_3}\right) \left(S + \frac{1}{\tau_4}\right)} .$$

In order to obtain a stable response we must compensate the lag terms by lead terms. A tachometer would give us a $(1 + S\tau_1)$ term in the numerator, but this is still inadequate for good response. To achieve further compensation we use a servo motor in the feed back loop of a high gain amplifier. This has the property of inverting the transfer function in the feed back loop which gives us an additional $S\left(S + \frac{1}{\tau_2}\right)$ term in the numerator. The over-all transfer function is then of the form

$$\frac{K}{S} \quad \frac{\left(S + \frac{1}{\tau_1}\right)}{\left(S + \frac{1}{\tau_4}\right)} \quad \frac{\left(S + \frac{1}{\tau_2}\right)}{\left(S + \frac{1}{\tau_3}\right)} .$$

By suitable choice of τ_1 and K an acceptable dynamic response can be achieved.

Fig. 2a shows the simplified block diagram of the control circuit. The rated speed of the drum is 4000 RPM. Let β be the phase error of the square wave. The electromechanical part of the drum synchronizer translates the phase error β into a shaft rotation of 15β which is the phase error of the system with respect to the 1000 cps reference.

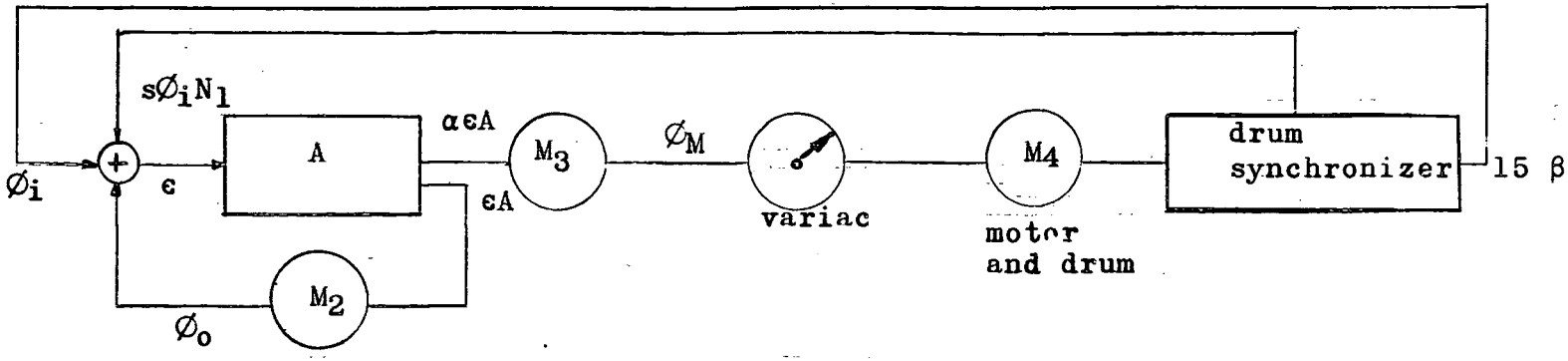

(a) Simplified Block Diagram of Servo Loop

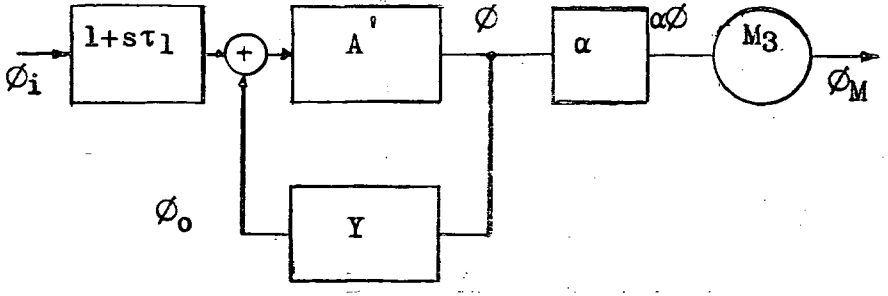

(b) Transferfunction $\frac{\phi_M}{\phi_i}$

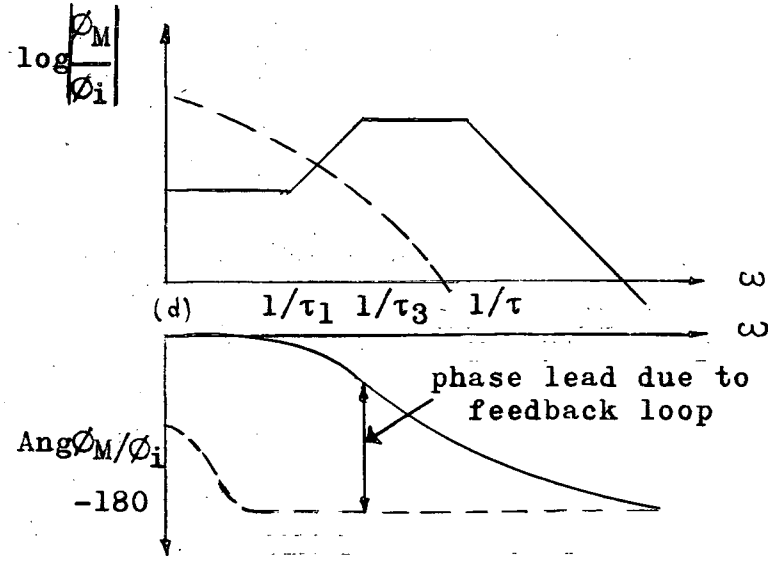

(c) Asymptotic Plot of ϕ_M/ϕ_i

Figure 2

Because the drum has a relatively large time constant compared with the Drum Synchronizer, the Drum Synchronizer will position rapidly to the phase error. The Drum Synchronizer has also an output proportioned to $\frac{d\phi_i}{dt} = S\phi_i$ which is used to improve the performance of the system. The output of the amplifier is fed to the motors M_2 and M_3. The feed back loop containing M_2 is used to stabilize the system. The reactions of the motor M_2 are opposing those of the drum; therefore M_2 helps to make the over-all operation stable. The motor M_3 rotates a variac which in turn changes the input voltage of the drum motor.

We will now apply linear analysis as a guide in determining the compensating elements to achieve system stability.

Let J be the moment of inertia of all rotating parts at the output shaft

f the coefficient of viscous friction referred to the output shaft

k_2 and k_3 proportionality coefficients referring to motor M_2 and M_3 respectively

k_s the synchro displacement constant in volts/rad

k_t the tacho speed constant in volts/rad/sec

α the step-up ratio of the output transformer

k_v variac displacement constant in volts/rad

N_1, N_2, N_3, gear ratio

b, d, scaling factors

A the amplifier gain

Then $\epsilon = dk_s \quad (\emptyset_i - \emptyset_o) + bk_t \; N_1 \; S \; \emptyset_i$,

$$\epsilon = dk_s \left[(1 + S \; \tau_1) \quad \emptyset_i - \emptyset_o \right]$$

with $T_1 = \dfrac{bk_t \; N_1}{dk_s}$ and $A' = A \; dk_s$.

With this, Fig. 2b is easily derived.

Therefore

$$\frac{\emptyset}{\emptyset_i} = (1 + S\tau_1) \; \frac{A'}{1 + A'Y},$$

$$\frac{\emptyset}{\emptyset_i} = \frac{\frac{1}{Y}}{1 + \frac{1}{A' \; Y}},$$

$$k_2\emptyset = J_2 S \; (S + \frac{1}{\tau_2}) \; \emptyset_o,$$

where $\tau_2 = \dfrac{J_2}{k_2}$.

Hence $Y = \dfrac{\emptyset_o}{\emptyset} = \dfrac{k_2}{J_2} \; \dfrac{1}{S(S + \frac{1}{\tau_2})}$,

$$\frac{\emptyset}{\emptyset_i} = \frac{J_2}{k_2} \; (1 + S\tau_1) \; \frac{S(S + \frac{1}{\tau_2})}{1 + \frac{J_2}{A'k_2} S(S + \frac{1}{\tau_2})}.$$

From Fig. 2b

$$\alpha k_3\emptyset = J_3 S(S + \frac{1}{\tau_3}) \; \emptyset_M,$$

$$\frac{\phi_M}{\phi} = \frac{k_3}{J_3} \quad \alpha \quad \frac{1}{S(S + \frac{1}{\tau_3})} \quad .$$

Therefore

$$\frac{\phi_M}{\phi_i} = \alpha \left(\frac{k_3}{k_2}\right) \left(\frac{J_2}{J_3}\right) \frac{(S + \frac{1}{\tau_2})}{(S + \frac{1}{\tau_3})} \quad \frac{(1 + S\tau_1)}{1 + \frac{J_2}{k_2} \frac{1}{Adk_s} S(S + \frac{1}{\tau_2})} .$$

The type of frequency response to be expected is shown in Fig. 2c and 2d. τ_1 is assumed to be zero, $\frac{1}{\tau_2}$ is smaller than $\frac{1}{\tau_3}$ ω bigger than $\frac{1}{\tau}$ defines the high frequency range in which the feed back loop loses its stabilizing effect.

The dotted lines indicate the response with the compensating feed back loop removed. With this type of compensating network we can expect to obtain a large phase lead between $+90^\circ$ and $+180^\circ$ over the useful range of operation of the system.

The part of the loop formed by A, M_2, and M_3 is non-linear due to the amplifier saturation and the non-linear motor characteristics. We can use the describing function method to characterize the transfer function which is now a function of input amplitude. The describing function method relates the fundamental components of the output to a sinusoidal input and neglects all higher harmonic outputs. The transfer function from the synchro input to the variac output is replaced by the describing function $G(S,\phi_i)$. $G(S,\phi_i)$ was measured experimentally for $\phi_i = 30^\circ$, 12°, 4.5°, and 1.5°.

Let β be the phase error of the square wave, then

$$(J_4 S^2 + f_4 S)\ \beta = k_o \quad k_v\ \phi_M = k_o \Delta V.$$

Therefore $$\frac{\beta}{\phi_i} = \frac{\beta}{\phi_M} \times \frac{\phi_M}{\phi_i} = \left(\frac{k_o}{J_4}\right)\ G\ (S, \phi_i)\ \frac{1 + S\ \tau_1}{S(S + \frac{1}{\tau_4})}\ .$$

$\frac{k_o}{J_4}$ will be calculated from the steady state voltage and current as a function of the angular velocity of the drum. The tachometer determines τ_1 and is used to increase the stability of the system in addition to providing the required frequency control.

THE EVALUATION OF THE DRUM CONSTANTS

To evaluate the drum constants consider the series AC-DC drum drive motor M_4.

Let V_m be the voltage drop due to the counter e.m.f.

V the voltage applied to the motor

Z the impedance of the Motor M_4

Ω the angular velocity of the motor.

The relationships between the above quantities are as follows:

$$V_m = kI\Omega ,$$

$$V = I\,(Z + k\Omega).$$

From which $$I = \frac{V}{Z + k\Omega} .$$

The useful torque of the motor is

$$T = \text{Const. } I\emptyset = k_4 \left| I \right|^2$$

where $\emptyset$ is the magnetic flux.

Therefore $T + k_4 \left| \frac{V}{Z + k\Omega} \right| 2.$

Let V_{ss} and I_{ss} be the steady state values which are functions of Ω . $T = T_{ss}$ is then the steady state torque required to drive the drum at a constant speed.

Therefore $$(Z + k\Omega) = \frac{V_{ss}}{I_{ss}} ,$$

$$T = k_4 \left| \frac{I_{ss}}{V_{ss}} \right|^2 \left| V \right|^2 ,$$

$$T_{ss} = k_4 \left| I_{ss} \right|^2 .$$

But $T = T_{ss}$ + the available torque for accelerating the drum,

$$T = T_{ss} + J_4 \frac{d\Omega}{dt} .$$

Therefore $\frac{d\Omega}{dt} = \frac{1}{J_4} (T - T_{ss})$,

$$\frac{d\Omega}{dt} = \frac{k_4}{J_4} \left|\frac{I_{ss}}{V_{ss}}\right|^2 \left| V^2 - V_{ss}^2 \right| .$$

Let $f_1 (\Omega) = \frac{k_4}{J_4} \left|\frac{I_{ss}}{V_{ss}}\right|^2$

and $f_2 (\Omega) = \frac{k_4}{J_4} \left| I_{ss} \right|^2$.

Then $$\frac{d\Omega}{dt} = f_1 (\Omega) V^2 - f_2 (\Omega) . \qquad (1)$$

For convenience we also drop the absolute sign and consider all values to be effective values.

This equation is a general equation describing the dynamic response of the motor and drum. By considering small deviations from the steady state position we can linearize equation (1)

$$\frac{d\Delta\Omega}{dt} = f_1 (\Omega_{ss}) \, 2 \, V_{ss} \Delta V + \frac{\partial f_1 (\Omega)}{\partial \Omega} V_{ss}^2 \Delta\Omega - \frac{\partial f_2 (\Omega)}{\partial \Omega} \Delta\Omega . \qquad (2)$$

Comparing the above equation with the linearized equation

$$\frac{d\Delta\Omega}{dt} + \frac{\Delta\Omega}{\tau_4} = \frac{k_o}{J_4} \Delta V , \qquad (3)$$

gives $$-\frac{1}{\tau_4} = \frac{\partial f_1 (\Omega)}{\partial \Omega} V_{ss}^2 - \frac{\partial f_2 (\Omega)}{\partial \Omega} ,$$

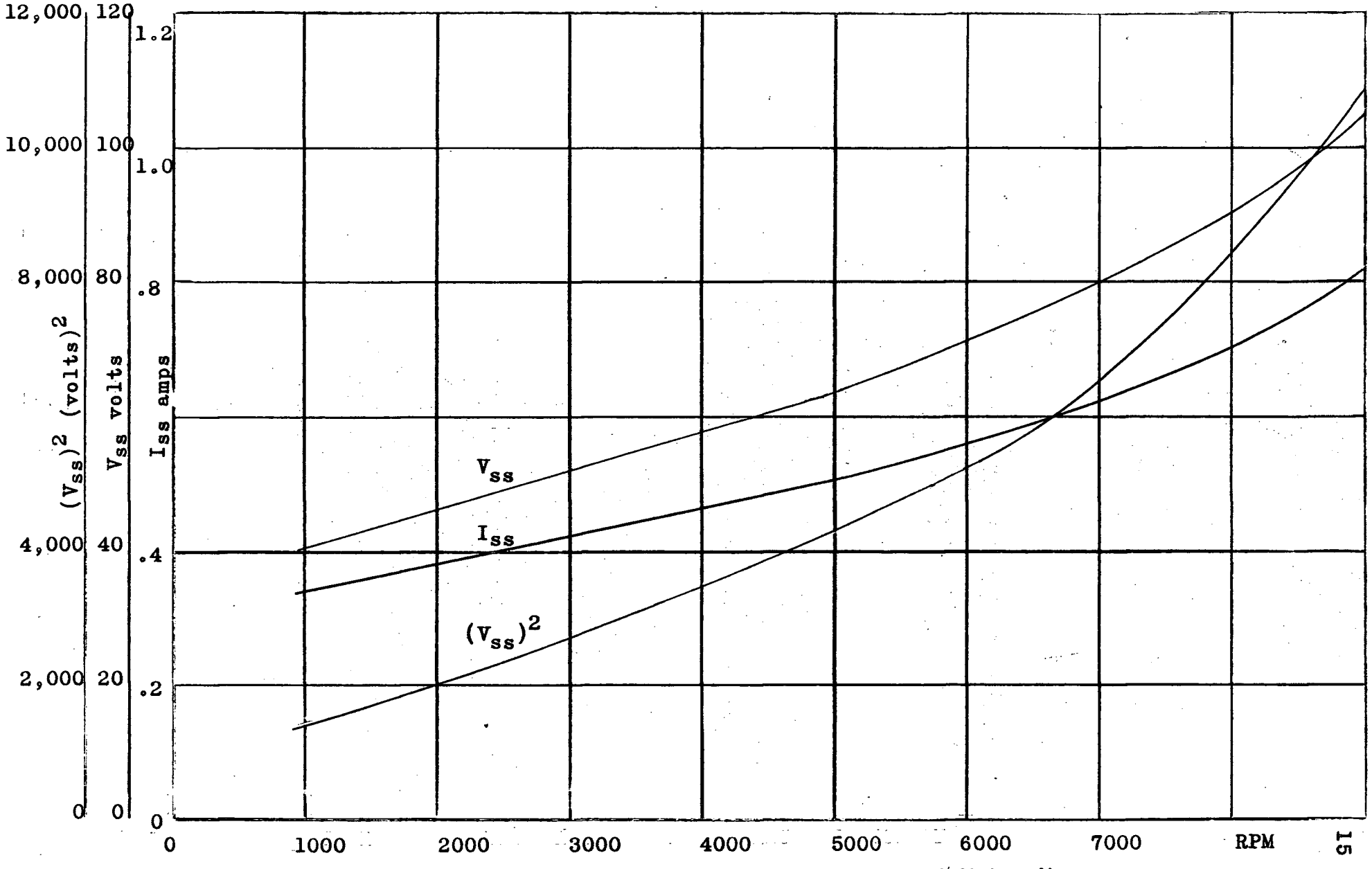

Figure 3. Current and Voltage Characteristics of Motor M_4

$$-\frac{1}{\tau_4} = \frac{k_4}{J_4}\left[V_{ss}^2 \frac{\partial}{\partial\Omega} \frac{(I_{ss})^2}{(V_{ss})^2} - \frac{\partial}{\partial\Omega} (I_{ss})^2 \right] .$$

After expanding

$$\frac{1}{\tau_4} = \frac{k_4}{J_4} \frac{(I_{ss})^2}{(V_{ss})^2} \frac{\partial}{\partial\Omega} (V_{ss})^2 ,$$

$$\frac{k_4}{J_4} = \frac{1}{\tau_4 \left(\frac{I_{ss}}{V_{ss}}\right)^2 \frac{\partial}{\partial\Omega} (V_{ss})^2} .$$

The time constant τ_4 was measured by observing the time required for the motor to reach 63% of the steady state speed for a voltage step of 3.0 volts at the rated speed of 4000 RPM.

$\tau_4 = 24.7$ sec/rad.

Fig. 3 shows T_{ss} and V_{ss} measured as a function of Ω. From the plot $(V_{ss})^2$ versus Ω at 4000 RPM (Fig. 3)

$$\frac{\partial}{\partial\Omega} (V_{ss})^2 = 7.64 \text{ (Volts)}^2 \frac{\text{sec}}{\text{rad}} ,$$

$$I_{ss} = 0.472 \text{ amps and}$$

$$V_{ss} = 58.7 \text{ volts at 4000 RPM.}$$

Also by comparing equation (2) and equation (3)

$$f_1 (\Omega_{ss})\, 2\, V_{ss} = \frac{k_o}{J_4} ,$$

$$\frac{k_o}{J_4} = 2\, V_{ss} \frac{k_4}{J_4} \frac{(I_{ss})^2}{(V_{ss})^2} ,$$

$$\frac{k_o}{J_4} = (2)\ (81.5)\ \frac{(0.472)^2}{58.7} = .620 \quad \frac{(\text{Rad})^2}{(\text{Sec})^2 \text{Volts}} \ .$$

Because $\Delta V = k_v \phi_M$,

$$k_v = \frac{115}{320} \times \frac{360}{2\pi} = 20.6 \ \frac{\text{Volts}}{\text{Rad}} \ ,$$

(for 115 volts applied to the variac)

equation (3) becomes

$$\frac{d\Delta\Omega}{dt} + \frac{\Delta\Omega}{24.7} = .620\,\Delta V = 12.78\ \phi_M$$

and

$$\Delta\Omega = \frac{12.78\ \phi_M}{S + \frac{1}{24.7}} \ . \tag{4}$$

It will be shown in Chapter III that the largest amplitude $\Delta V = \pm$ 66 volts was measured at the frequency 0.650 rad/sec. From that it follows that $\Delta\Omega = \pm$ 565 RPM.

From the plot V_{ss} versus Ω and I_{ss} versus Ω it can be concluded that for a change of Ω = 565 RPM the drum operates in a linear region. Therefore the transfer function of the drum may be assumed to be linear throughout the range of operation.

The open loop overall transfer function is

$$\frac{15\beta}{\phi_i} = Y_o(S,\phi_i) = 9.30\ G(S,\phi_i) \quad \frac{1 + S\,\tau_1}{S(S + \frac{1}{24.7})} \ . \tag{5}$$

This equation neglects the small phase shift in the drum synchronizer.

SERVO AMPLIFIER and STABILIZING LOOP

A shaft rotation ϕ_o of the servomotor M_2 will shift the rotating field in the synchro S_2 and S_1 by an amount proportional to ϕ_o. An additional rotation of the rotor of S_1 will produce an input voltage to the amplifier which is proportional to $\phi_i - \phi_o$. The addition of this voltage with the tachometer input, which is proportional to $S\phi_i$, will give an error voltage $e = dk_s(\phi_i - \phi_o) + bk_t S\phi_i$. It is assumed that the angles ϕ_o and ϕ_i are small. The error voltage e is a 60 cps amplitude modulated signal which is fed into a phase inverter. The output of the phase inverter gives two signals of equal amplitude but 180° out of phase. This signal is fed into a class AB push-pull power amplifier and from there through the output transformer to the motors M_2 and M_3.

The overall voltage gain of the phase inverter, amplifier, and output transformer for small voltages is 570. At approximately 400 mV RMS input the amplifier reaches saturation. The output voltage of the amplifier is nearly 90° out of phase with respect to the A.C. component of the plate current due to the predominantly inductive load. As a consequence of the pentode drive the output voltage is nearly 90° out of phase with respect to the input voltage. The voltage on the two servomotor windings are then approximately 90° out of phase. This is necessary for proper operation of the servomotors.

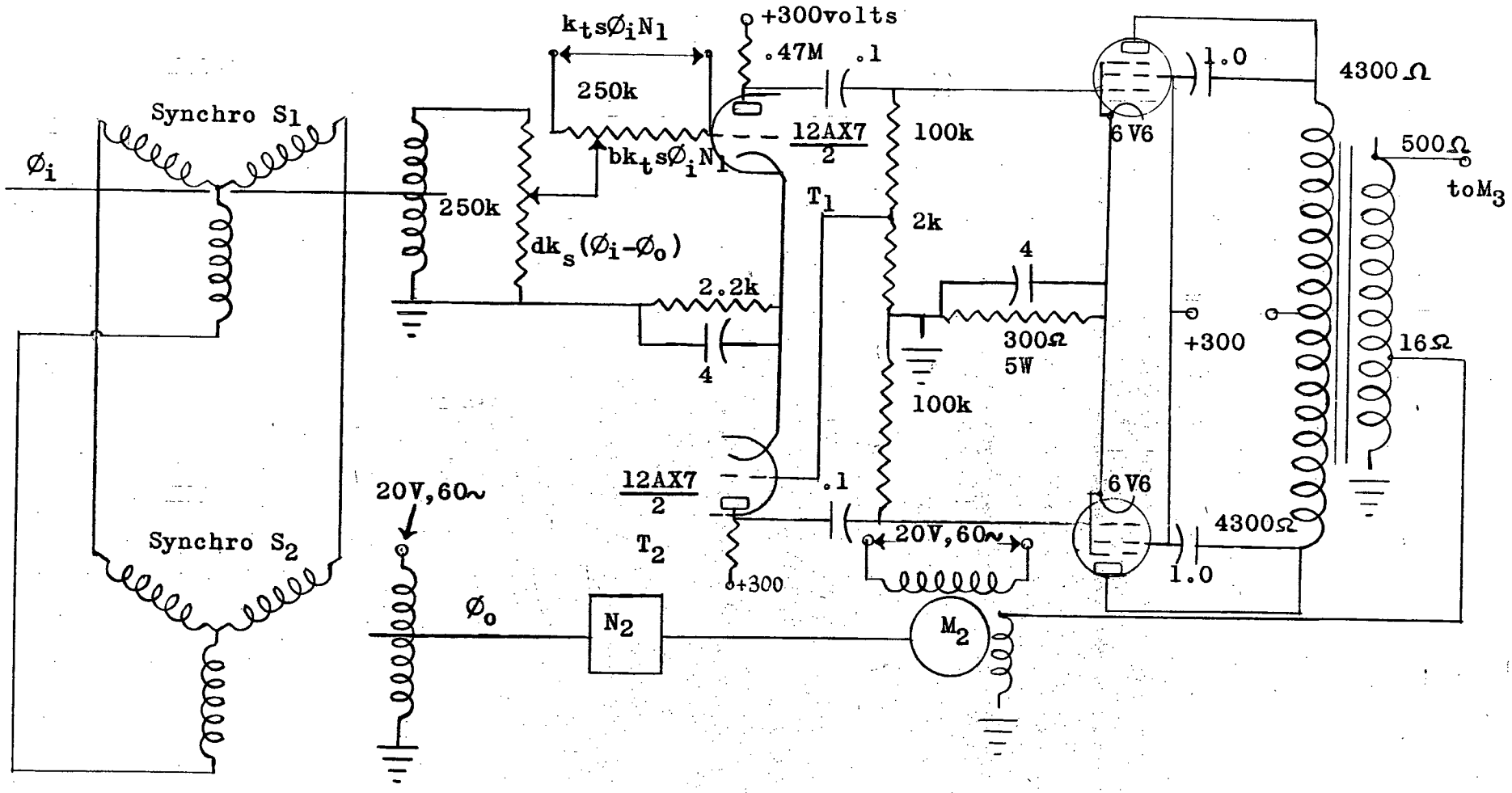

Figure 4. Servo Amplifier and Stabilizing Loop

Any error voltage will turn the servomotor M_2 until $\phi_i - \phi_o$ is equal zero.

Phase Inverter and Push-Pull Amplifier

In the two tube paraphase amplifier one tube is used as a conventional amplifier, the second tube is used as a phase-inverter amplifier. The ratio of the 100k and 2.0k resistance voltage divider across the output is chosen so that the gain from the anode of T_1 to T_2 is unity. To achieve proper phase inversion the 2.0k resistor is critical.

The push-pull amplifier is a conventional class AB audio amplifier. To cancel out the odd harmonic distortion due to an unbalance between tubes the cathode resistor was by-passed. Slight harmonic distortions do not influence the operation of the motors because a two phase motor acts like a filter with respect to the higher harmonics.

CHAPTER III

THE DRUM SYNCHRONIZER

Figure 5 shows the block diagram of the drum synchronizer. There are 1560 notches on the synchronizing track. Each track of the drum is divided into 15 channels, each channel corresponding to 104 notches on the synchronizing track. The output of the synchronizing track is almost sinusoidal. This wave form is amplified in a resistance-capacitance coupled amplifier and then fed into a peaker. Two phantastron dividers are used to divide the 104×10^3 pulses/sec by 8x13 = 104. The differentiated outputs of the dividers are taken from the cathode. The negative peaks of the second divider trigger a monostable multivibrator, the output of which is to be 1000 cps for proper operation. The phase of the output of the monostable multivibrator is compared with the 1000 cps standard in the phase sensitive rectifier.

The first harmonic of the square wave will be of the form $A \sin(\omega_c t + 15\beta)$ where β is the phase error of the square wave and ω_c is $(2\pi) \times (1000)$ rad/sec. The signal coming from a 1000 cycle tuning fork oscillator is fed through a resolver, the output of which is $B \sin(\omega_c t + \phi_i)$. ϕ_i is the angular position of the resolver rotor which is driven by the motor M_1. The phase sensitive rectifier produces a DC signal which is proportional to $(\phi_i - 15\beta)$ for small errors. This is chopped into a 60 cycle error signal and by means of the power amplifier produces a torque on the rotor of the motor M_1.

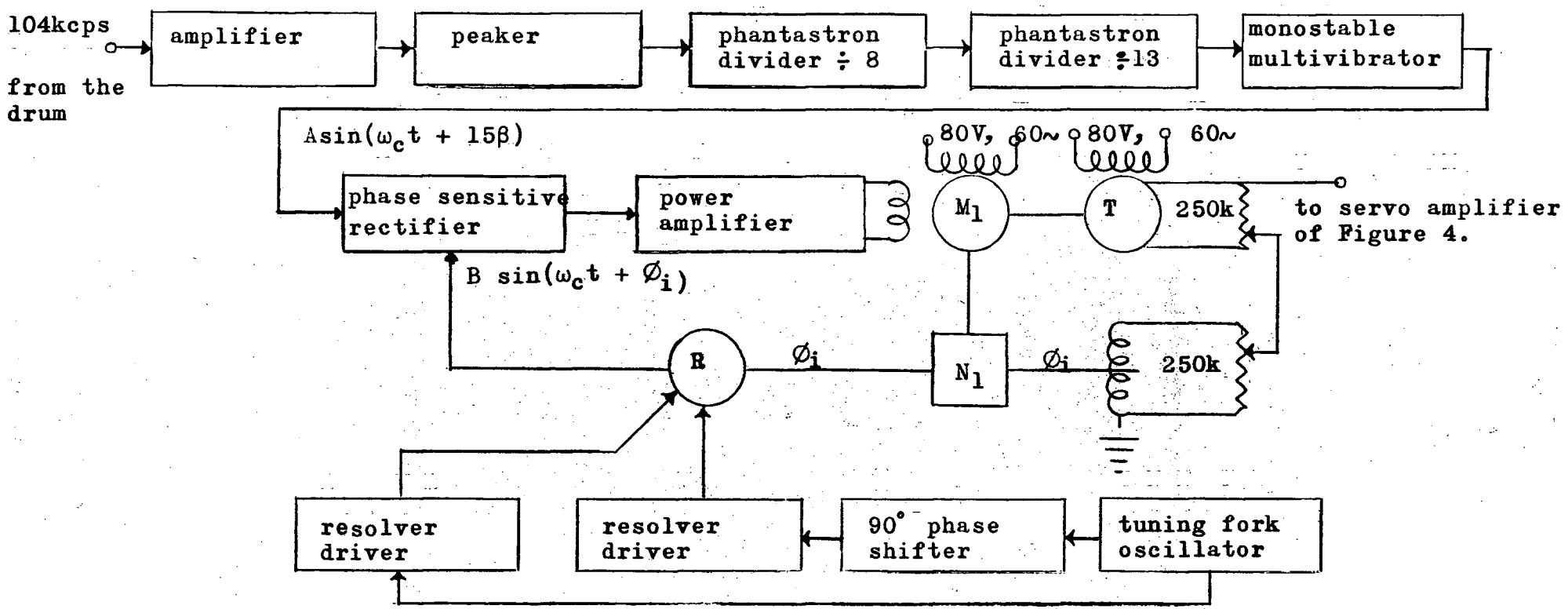

Figure 5. Block Diagram of Drum Synchronizer

M_1 will position rapidly due to the fast response of the motor. The dynamic operation of the system can be visualized in the following manner: (See Fig. 4.)

The phase error $\epsilon = \phi_i - 15\beta$ will cause M_1 to position until $\epsilon = 0$. The synchro S_1 and the tachometer transmit driving voltages to M_2 and M_3. M_2 positions S_2 to cancel this voltage and M_3 stops. The end effect is that the variac has moved a small amount. This causes a change in torque of the drum drive motor which reduces β.

Amplifier and Peaker

The input to the resistance-capacitance coupled amplifier is approximately a sinusoidal signal of 250 mV peak to peak and the frequency is about 104 kcps. The voltage gain of the amplifier is 70. The peaker is essentially a R-L differentiating network. The diode clips the positive going pulses. The resistance in series with the diode provides a constant voltage output during the conduction interval of the diode.

PHANTASTRON DIVIDER

The phantastron divider is a type of monostable trigger circuit. It differs from a multivibrator mainly in the fact that a linear time wave form is used rather than the exponential in multivibrators. This increases the precision since the linear sweep is not very much affected by the tube characteristics.

Consider the cathode coupled phantastron shown in

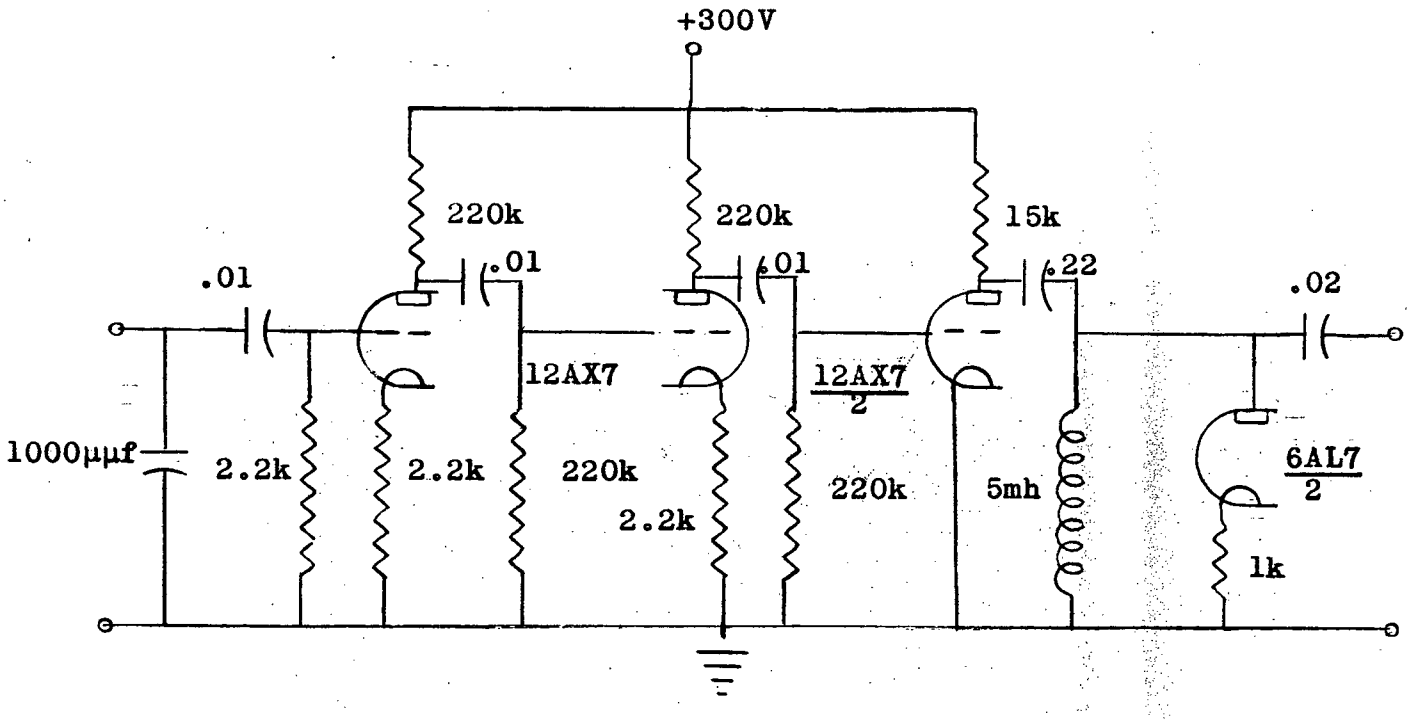

Figure 6. Amplifier and Peaker

Fig. 7a. Under normal conditions with the plate current cut off by the suppressor, the plate voltage will be E_{cc} because it is held at that potential by T_3. The resistance voltage divider network and the conducting diode T_2 set the grid level at E_D volts.

These are the circuit conditions existing just prior to the incidence of a negative gate on the plate. A negative input pulse of about 30 volts is applied to the plate of T_1 through T_3. As the plate of T_1 drops regeneration starts which disconnects T_1 from further signal pulses. Because of the action of the feed-back capacitor C the grid drops by an equal amount as the plate, thereby becoming negative. The drop of the plate voltage is stopped by the action of the grid. Once this equilibrium is established, conventional Miller integration in a class A amplifier occurs through C and Rg. During this initial change the screen current is very much reduced because the tube is now operating as a pentode. Therefore the screen voltage rises rapidly at the beginning of the sweep. The plate voltage is falling almost linearly as a function of time. The grid voltage rises only slightly during this period to compensate for the increase of plate current. When the plate voltage bottoms the grid voltage rises rapidly toward E_{gg} as C charges.

When the grid rises so does the cathode. This makes the suppressor negative with respect to the cathode. The plate current is cut off and the screen potential drops. The positive

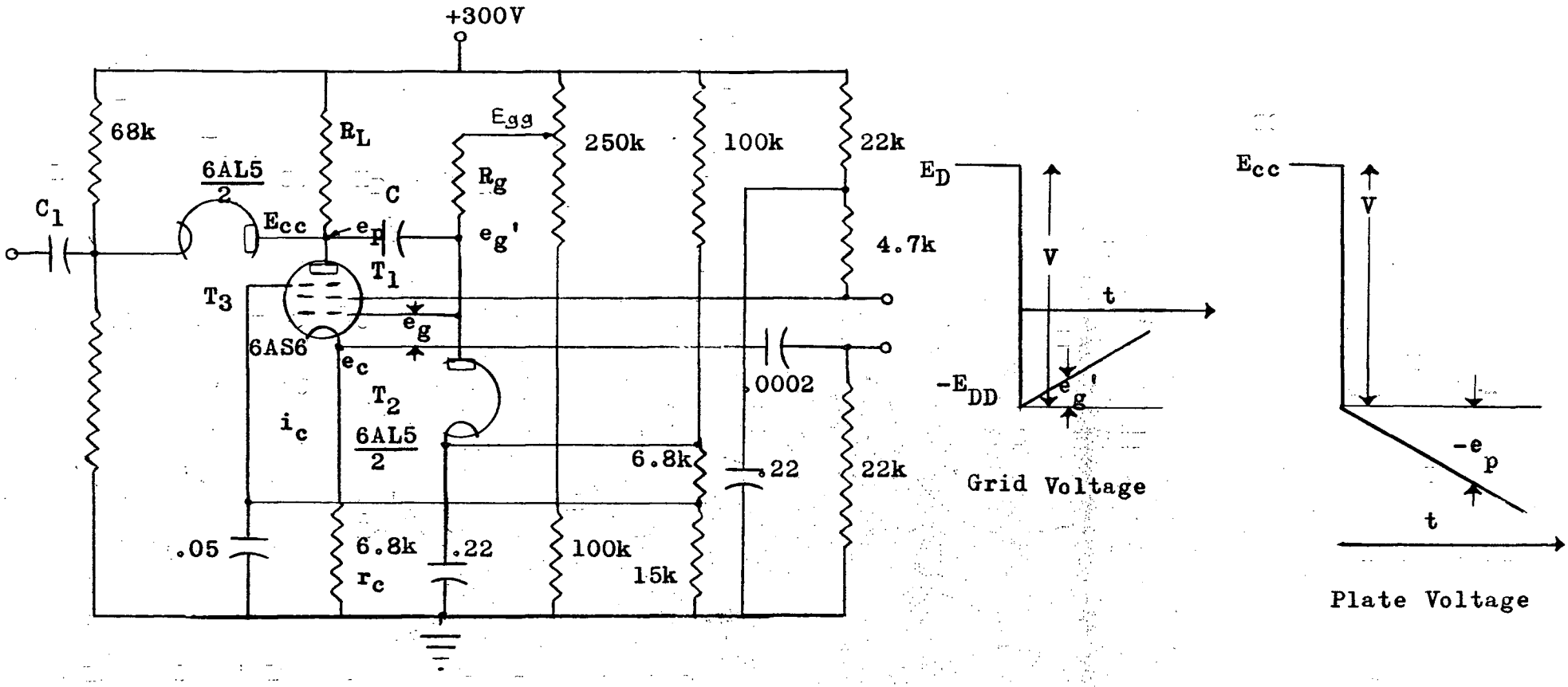

104kcps ÷ 8=13kcps
R_L=68k
R_g=3M
C=50μμf
C_1=.02μf

13kcps ÷ 13=1kcps
R_L=68k
R_g=6.9M
C=250μμf
C_1=.05μf

(a) Phantastron Divider

(b) Grid and Plate Voltages during the Sweep

Figure 7

rise of the grid is stopped when T_2 conducts. Then the plate rises toward E_{pp} with a speed mainly determined by $R_L C$. The plate potential rises until T_3 conducts. As soon as a pulse appears on the cathode of T_3 the action will be repeated.

Phantastron Analysis

The division ratios of 8 and 13 must be stable. It is therefore important to know the effect of tube variations on the division stability.

For the 6AS6 pentode used the division ratio of plate to screen current during the sweep is approximately 3:1. Referring to Fig. 7a and b we have

$$i_c = \frac{4}{3} i_p ,$$

$$e_g = e_g' - i_c r_c ,$$

$$i_p = g_m e_g ,$$

$$- e_p = g_m R_L e_g .$$

Therefore $$e_g \left(1 + \frac{3}{2} g_m r_c\right) = e_g' .$$

The current flowing through the condenser is

$$\frac{E_{gg} + E_{DD} - e_g'}{R_g} = C \frac{d}{dt} (e_g' - e_p) .$$

E_{DD} is defined by $-E_{DD} = E_D - V$ where V is the initial step in plate voltage. $E_{gg} + E_{DD} = SR_g (-e_p) + e_g' (1 + SCR_g)$

Let $C R_g = \tau$,

$$E_{gg} + E_{DD} = -S\tau e_p + (1 + S\tau)\left(1 + \frac{4}{3} g_m r_c\right)\left(\frac{-e_p}{g_m R_L}\right) ,$$

$$-(E_{gg} + E_{DD}) = e_p\left[\left(1 + \frac{1}{g_m R_L} + \frac{4}{3}\frac{r_c}{R_L}\right)(S\tau) + \frac{1}{g_m R_L} + \frac{4}{3}\frac{r_c}{R_L}\right] .$$

With $\frac{r_c}{R_L} = 0.1$, $g_m = 3.2 \times 10^{-3}$, and $\frac{1}{g_m R_L} \approx 0$,

$$e_p(s) \cong \frac{-(E_{gg} + E_{DD})}{(1 + \frac{4}{30})s\tau + \frac{4}{30}} ,$$

$$e_p(s) \cong \frac{(-30)(E_{gg} + E_{DD})}{4(1 + \frac{34}{4}s\tau)} ,$$

$$-e_p(t) \cong \frac{30}{4}(E_{gg} + E_{DD})(1 - e^{-\frac{4}{34}\frac{t}{\tau}}) ,$$

$$-e_p(t) \cong \frac{30}{4}(E_{gg} + E_{DD})\frac{4}{34}\frac{t}{\tau} .$$

The linear sweep is terminated when

$$-e_p = E_{cc} - (V + V_b + E_c),$$

where V is the initial voltage step, V_b is the bottoming potential of the tube, and E_c the cathode potential with respect to ground at the time of bottoming.

Therefore $$t = \frac{34}{30}\tau\frac{E_{cc} - (V + V_b + E_c)}{E_{gg} + E_{DD}} .$$

But $$V = E_D + E_{DD}$$

and $$t = \frac{E_{cc} - (E_D + E_{DD} + V_b + E_c)}{E_{gg} + E_{DD}} .$$

E_{DD}, V_b, and E_c will change with variation in tube parameters. Therefore

$$\frac{\Delta t}{t} \cong - \frac{(\Delta E_{DD} + \Delta V_b + \Delta E_c)}{E_{cc} - (E_D + E_{DD} + V_b + E_c)} - \frac{\Delta E_{DD}}{E_{gg} + E_{DD}} .$$

Let the tube parameters vary $\pm$ 30%

$$\left|\frac{\Delta E_{DD}}{E_{DD}}\right| = \left|\frac{\Delta V_b}{V_b}\right| = \left|\frac{\Delta E_c}{E_c}\right| = 0.3 .$$

With $E_{DD} = 3$ volts, $E_D = 48$ volts ,

$V_b = 2$ volts, $E_{gg} = 138$ for a division ratio of 10,

$E_c = 25$ volts, $E_{cc} = 263$ volts ,

$$\left|\frac{\Delta t}{t}\right| = 0.048 = 4.8\% .$$

Therefore it may be concluded that the sweep time of the phantastron may change $\pm$ 4.8% with a variation of the tube parameters of $\pm$ 30%. This is acceptable for proper operation of the phantastron.

Phase Sensitive Detector and Motor Driving Stage

The output of the monostable multivibrator is a square wave of 30 volts peak to peak. It is fed into a cathode follower and used as a reference wave form.(Fig. 8) When the reference wave form is positive, the cathodes of the differential amplifier are raised and the tubes are cut off. During the negative part of the reference wave form the cathode follower does not conduct and the differential amplifier functions as an amplitude discriminating circuit. One grid is grounded, the other grid is supplied by the output of the resolver rotor, the voltage of which

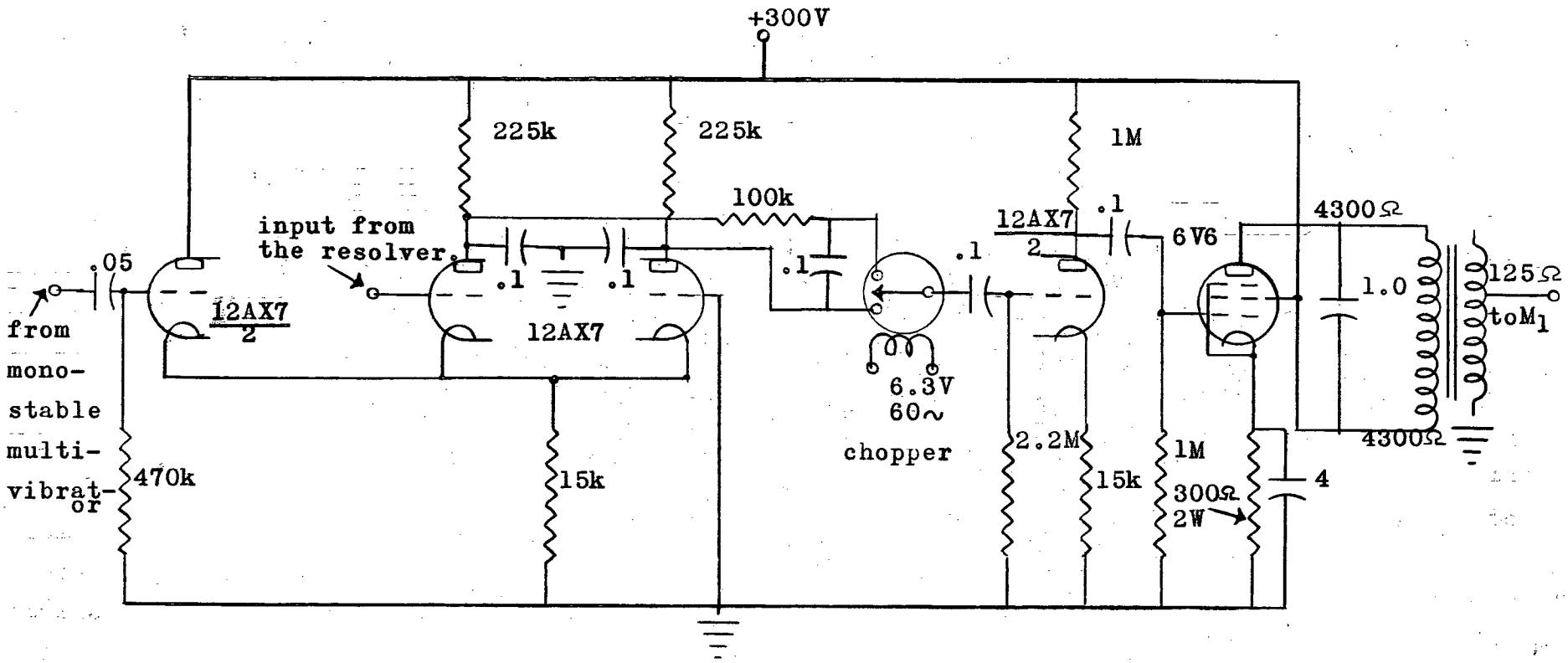

Figure 8. Phase Sensitive Rectifier and Motor Driving Stage

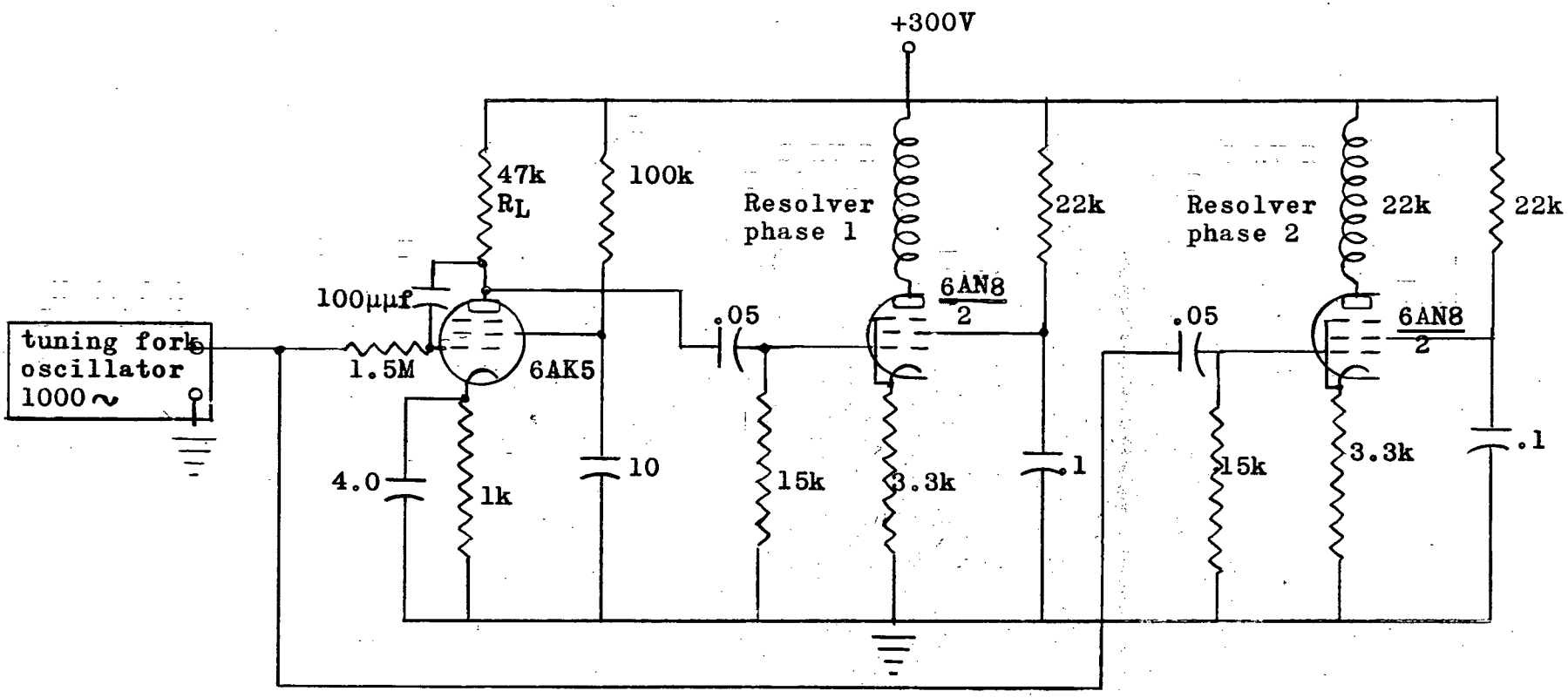

Figure 9. Phase Shifter and Resolver Drivers

is approximately 1 sin $(\omega_c t + \phi_i)$ volts; ω_c is the carrier frequency (2π) (1000) rad/sec. The common cathode resistor provides almost balanced push-pull grid-cathode voltages.

The phase error is then proportional to the DC voltage difference between the plates. The time constant of the plate circuit is chosen as a compromise between adequate filtering the 1000 cps harmonics and small lag in the DC voltage following phase changes. The 100K resistor is a current limiting resistor to provide proper operation of the chopper. The differential amplifier should be approximately balanced.

The DC error signal is chopped into a square wave signal which is voltage amplified and then fed into the power amplifier which drives the motor M_1. The primary of the transformer is tuned approximately to the fundamental of the square wave.

The motor M_1 will turn until $\phi_i = 15\beta$. The synchro S_1 and the tachometer T are driven by M_1 and produce an error signal proportional to ϕ_i and $s\phi_i$. Those signals are summed in the servo amplifier in order to correct for the error β in the drum position.

The gear ratio N_1 was chosen to be 27:1. If N_1 is chosen much larger the motor M_1 will not be able to follow frequency errors. If N_1 is chosen much smaller the smoothness of the phase control will suffer.

<u>Monostable Cathode Coupled Multivibrator</u>

Consider Fig. 10. Normally T_2 is conducting and T_1 is cut off. A negative trigger will cut off T_2 and cause T_1

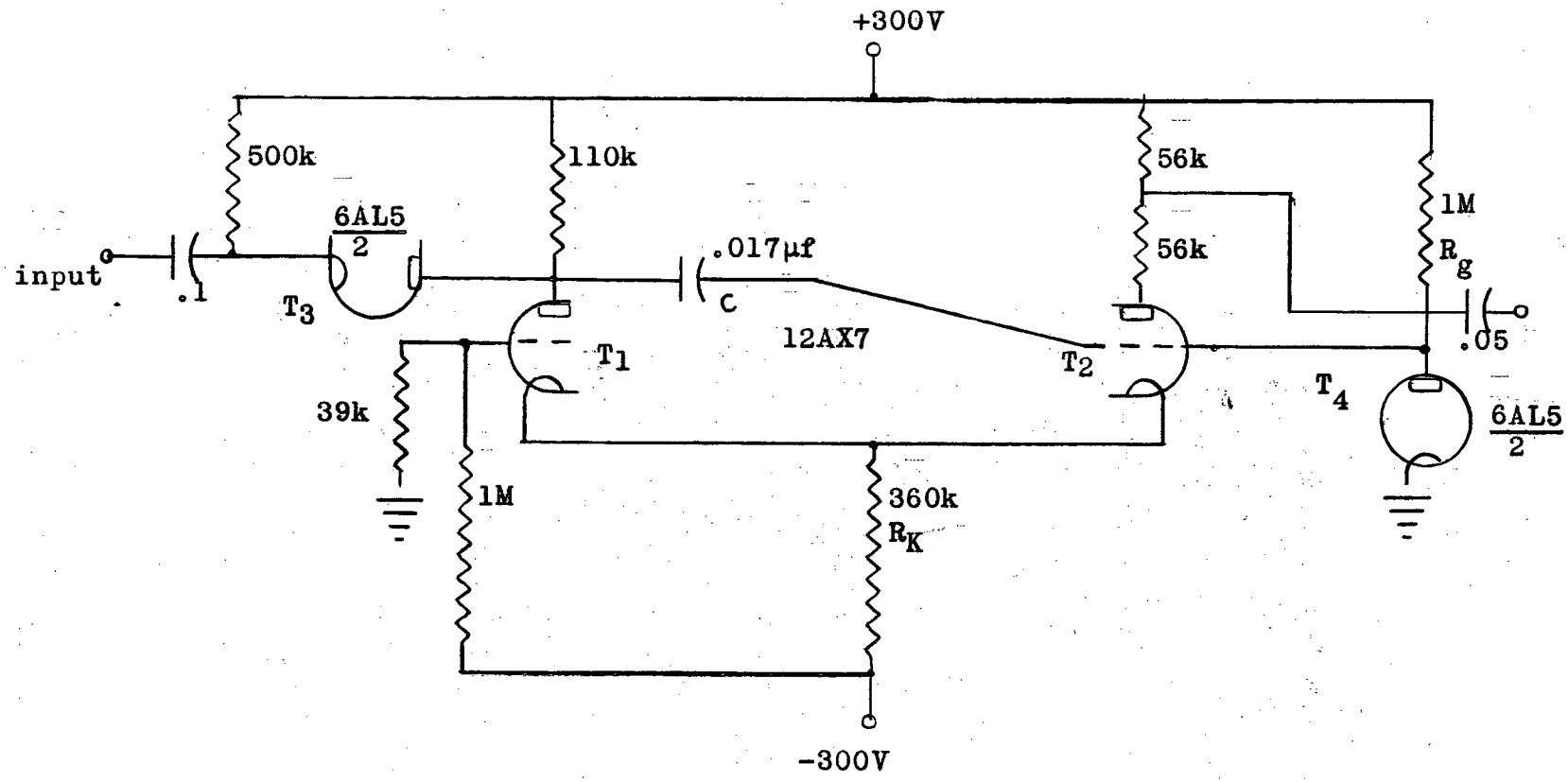

Figure 10. Monostable Cathode Coupled Multivibrator

to conduct. The plate of T_1 drops and keeps T_2 cut off. The grid of T_2 rises with a time constant mainly dependent on R_gC. When T_2 starts to conduct regeneration rapidly cuts off T_1. The circuit elements are chosen to give a recovery time of 1/2 millisecond. The output is then a square wave with a repetitive rate of 1000 cycles per second.

CHAPTER IV

Experimental Determination of the Describing Function $G(s,\phi_i)$

The system transfer function can not be represented as a function of s because it is non-linear for large inputs and large variations in motor speed. This is due to amplifier saturation and non-linear motor characteristics. The describing function is the system transfer function of the form $G(s,\phi_i)$.

Fig. 11 shows the experimental procedure for measuring the transfer function for part of the system. The input signal is obtained from the synchro S_4 through the synchro generator S_3. The motor M runs at a frequency f_s which represents the signal frequency. The output signal is obtained from the synchro S_6 and is applied to the Y plates of a C.R.O. The input, phase shifted through synchro S_5, is applied to the X-plates. The phase is adjusted until an approximate straight line is produced. The stability of the line indicates small harmonic components, and this justifies taking amplitude readings directly from the output shaft.

In carrying out the experiment synchro S_6 must be set to give zero output for $\phi_M = 0$. Otherwise the output signal is no longer 100% modulated and the straight line becomes an hour glass type pattern. Due to the non-linear friction effects, the average position of ϕ_M drifts slowly and the readings are best taken at the instance when the

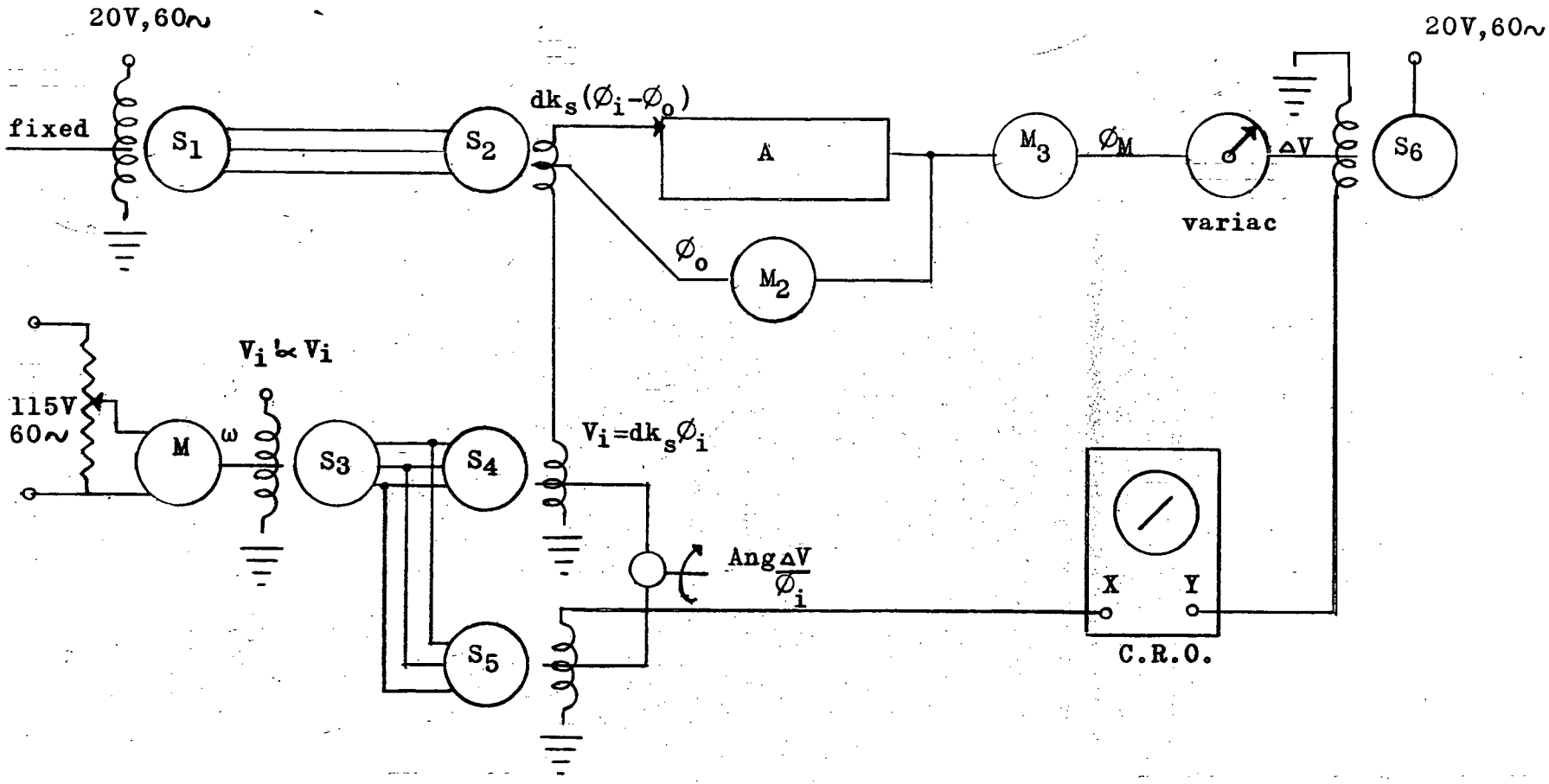

S_1, S_2 synchros
S_3 selsyn generator

S_4, S_5, S_6 selsyn control transformer
M series motor

Figure 11. Test Procedure for Measuring Gain Characteristics and Phase Shift of the Nonlinear Portion of the Servo System

modulation is 100%.

ϕ_M is measured for a given V_i at various frequencies. Because of erratic mechanical friction effects, very low frequency readings were not taken. ϕ_i and ΔV are easily calculated. Fig. 11 shows the plots of log $\frac{\Delta V}{\phi_i}$ versus ω for various ϕ_i's with τ_1 equal to zero.

$$\log \left|\frac{\Delta V}{\phi_i}\right| = \log \left|\frac{k_v \phi_M}{\phi_i}\right| = \log \left| G(S,\phi_i) \right| .$$

Fig. 12 shows a number of plots of $G(S,\phi_i)$. The over-all transfer function $Y_o(S,\phi_i)$ is then calculated from the equation.

$$Y_o(S,\phi_i) = 9.30\, G(S,\phi_i) \frac{\tau_1(S + \frac{1}{\tau_1})}{S(S + \frac{1}{24.7})} .$$

Fig. 13 shows the plots of $Y_o(S,\phi_i)$ and Fig. 14a shows the Nyquist diagrams of $Y_o(S,\phi_i)$ provided $\tau_1 = 0$.

From the Nyquist diagram it is obvious that the closed loop will be unstable. In order to make the system stable the gain of the system has to be decreased. We are also free to choose τ_1.

The system can be considered reasonably linear for small ϕ_i. From the general shape of the gain and phase characteristic of $Y_o(S,\phi_i)$ it can be concluded, as the amplifier saturates with increasing ϕ_i , that we obtain a larger phase lag and a reduced band width.

Let $\phi_i < 0.3$ radians and place the cut-off frequency

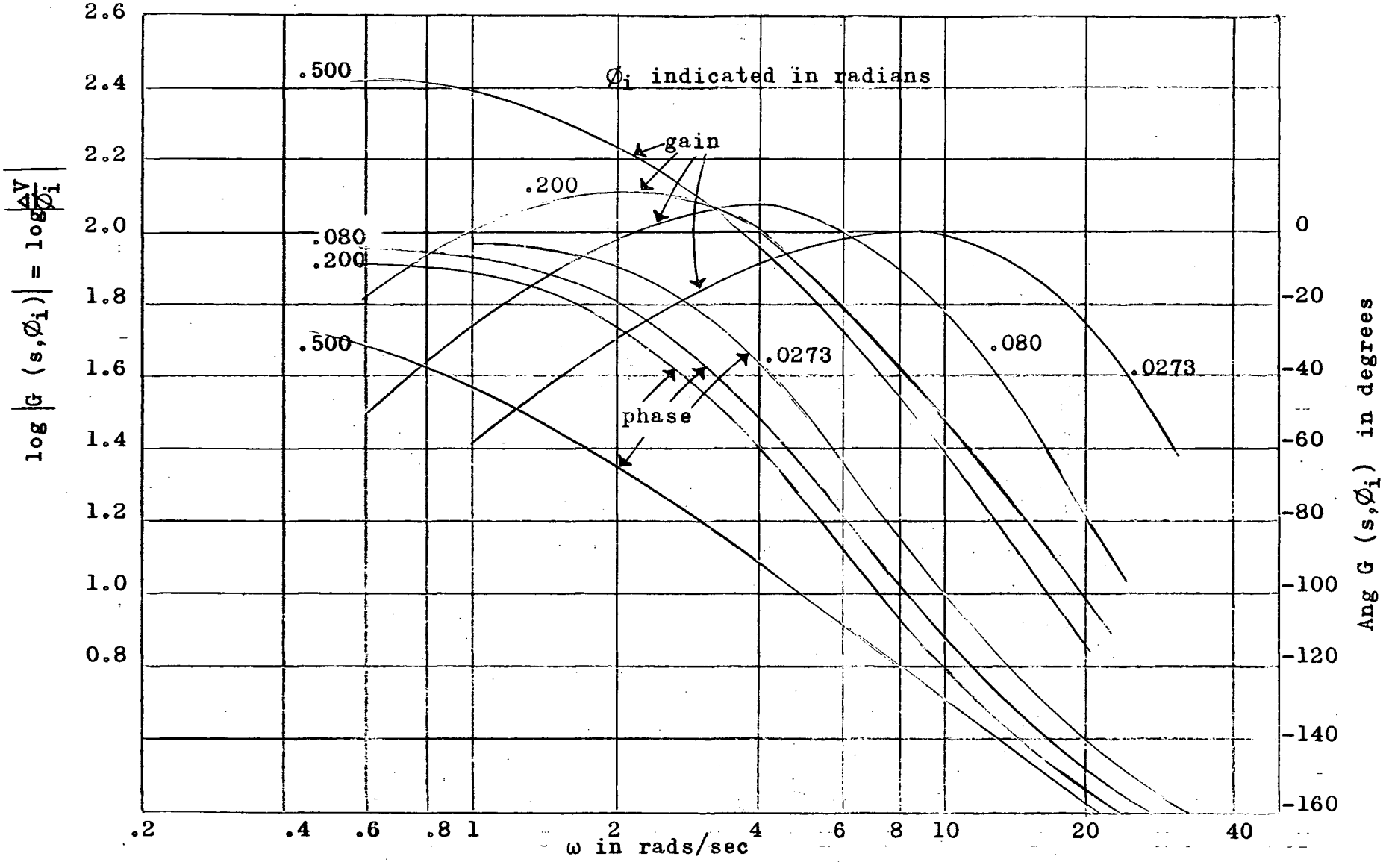

Figure 12. Gain and Phase Characteristics of the Non-linear Part of the Transfer Function

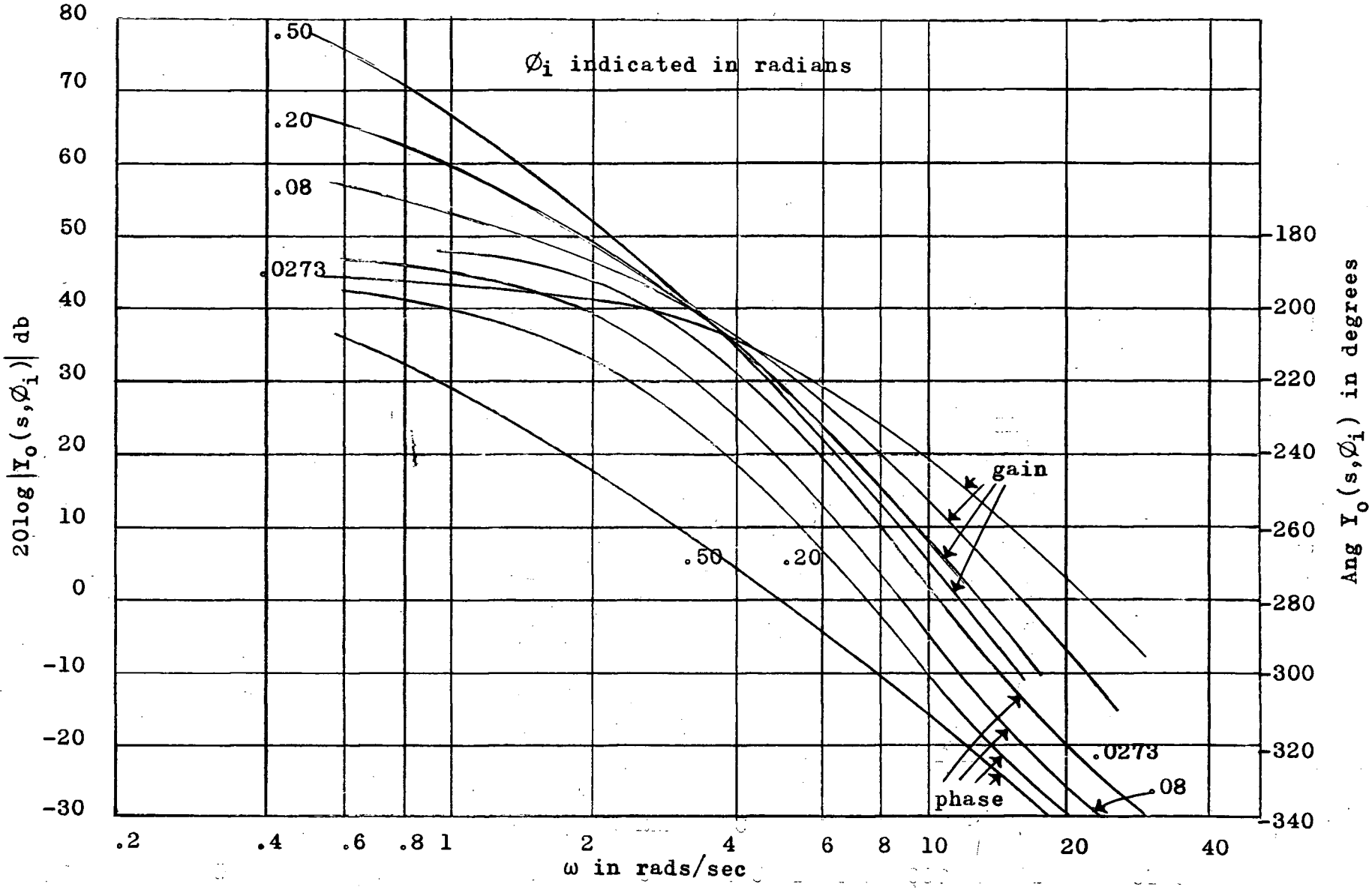

Figure 13. Gain and Phase Characteristics of Open Loop Transfer Function

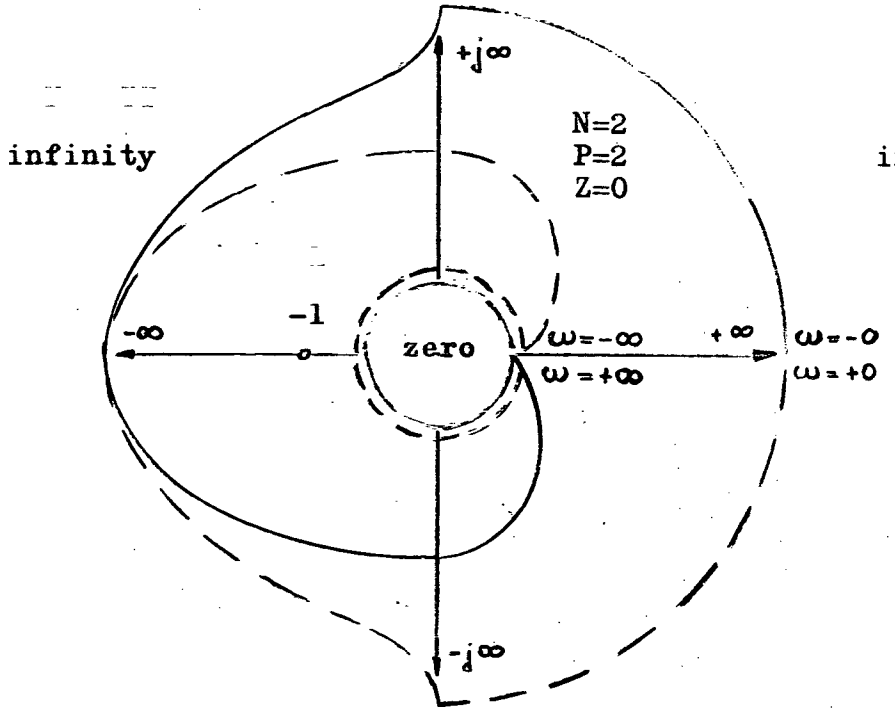

(a) $\frac{k_o}{J_4} \cdot \frac{G(s,\phi_i)_{\phi_i=\text{const.}}}{s(s+\frac{1}{\tau_4})}$

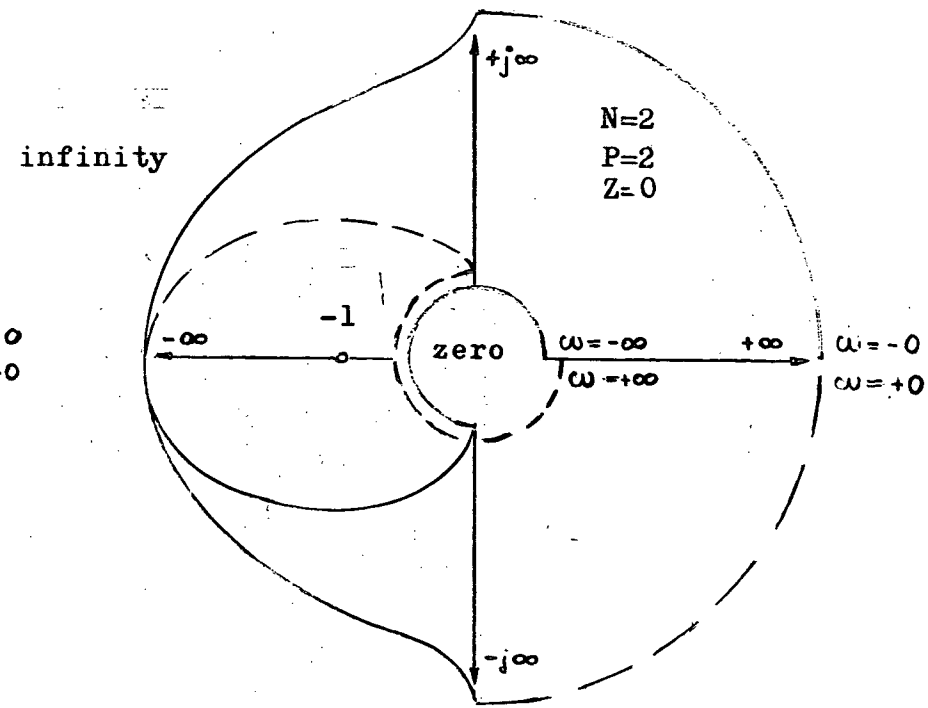

(b) $\frac{k_o}{J_4} \cdot \frac{(1+s\tau_1)\,G(s,\phi_i)_{\phi_i=\text{const.}}}{s(s+\frac{1}{\tau_4})}$

Figure 14. Nyquist Diagram (general shape)

at 2 rad/sec. In order to establish a phase margin of about 45° at the cut-off frequency choose $\tau_1 = 1/2$ rad/sec.

Because $k_t = 6.2 \frac{\text{Volts}}{1000 \text{ RPM}} = 5.92 \times 10^{-2} \frac{\text{Volts}}{\text{Rad/Sec}}$,

$$\tau_1 = \frac{b\, k_t\, N_1}{d\, k_s},$$

$$N_1 = 27, \quad d = 1, \quad k_s = 11 \frac{\text{Volts}}{\text{Rad}},$$

$$b = 1/2 \times \frac{11 \times 100}{5.92 \times 27} \cong 4 .$$

Therefore the rate-generator signal has to be amplified by a factor of approximately 4 which is done by a step up transformer of 1:4. This would increase the gain of $Y_0(S,\phi_i)$ as plotted in Fig. 12 by the factor

$$\left| \tau_1 \left(S + \frac{1}{\tau_1}\right) \right| = 2 = 3 \text{ db at cut-off.}$$

In order to have cut off for all $\phi_i < 0.3$ rad at $\omega_c = 2$ rad/sec the gain should be decreased by a factor N.

$$20 \log_{10} N = 52+3,$$

therefore $N = 560$.

This gain reduction is accomplished by inserting a gear ratio of 108:1 between motor M_3 and the variac and also by a step-down transformer of approximately 5:1 between the 115 volt supply and the variac. Fig. 15 shows the modifications.

The closed loop transfer function is then stable provided $\phi_i < 0.3$ radians. Final adjustment of gain and

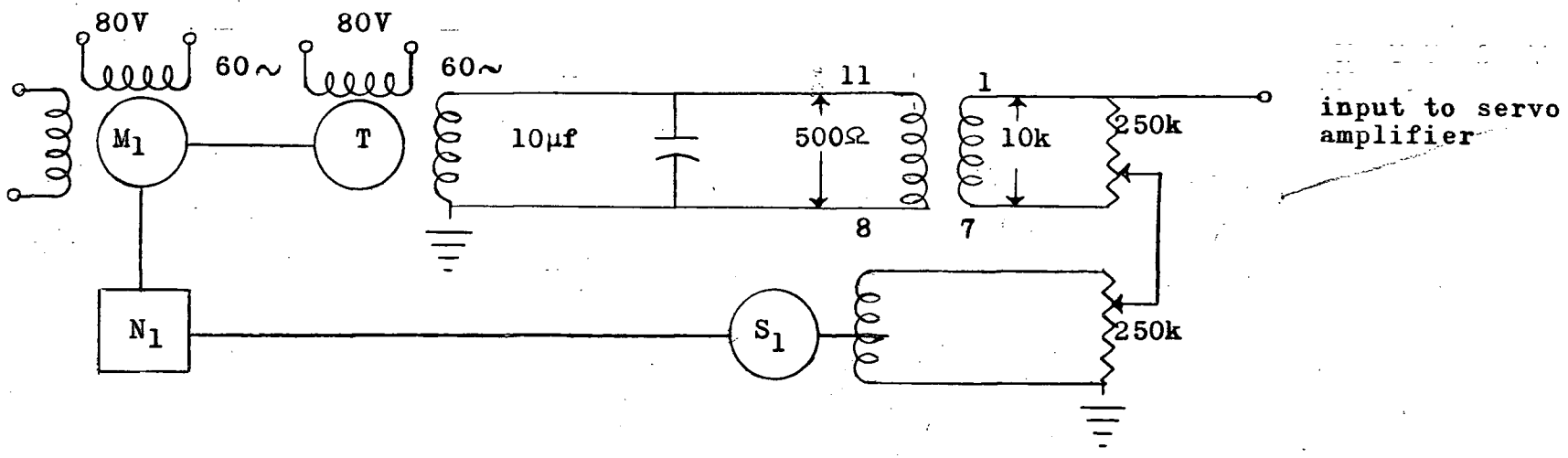

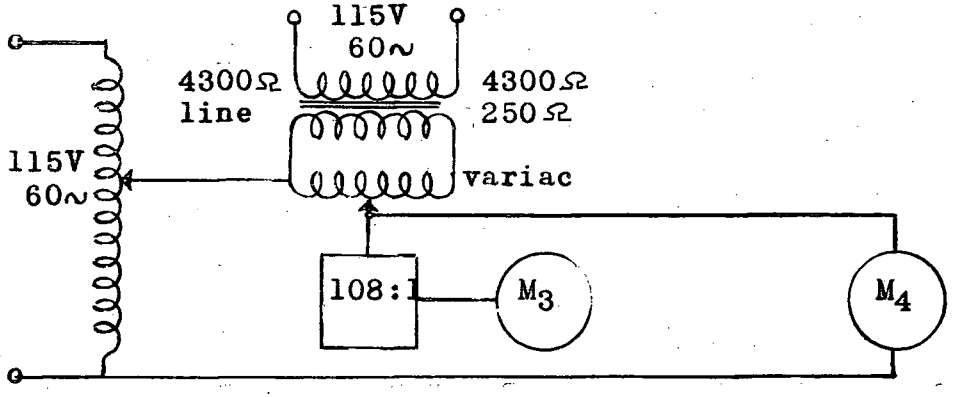

Figure 15. Circuit Modifications due to Stability Considerations

tachometer voltage is best done experimentally.

Test of the Over-all System

The various units of the control system were individually tested and operated satisfactorily. The loop was then closed. A rheostat was used to bring the drum up to the correct speed. Phase lock was achieved for brief intervals of a few seconds but the random frequency variations were larger than anticipated and the servomotor M_1 of the drum synchronizer was unable to follow. This servomotor was to supply a stabilizing signal from the tachometer and also a driving signal from the synchro S_1. Without adequate input signals the variac movement is not of sufficient amplitude to achieve a reliable phase lock. These tests indicated the need for a faster response and also the desirability of a greater frequency control region.

CHAPTER V.

REVISED DESIGN

The system requirements for a revised system are:

(1) A frequency control range to cover approximately $\pm$ 10 cps

(2) A phase control region with direct control of the variac.

To increase the frequency control region and to provide faster response the block diagram Fig. 16 was proposed. This system employs the same components except servo motors M_1 and M_2 have been eliminated.

The lead networks Y_1 and Y_2 are designed to introduce a phase lead up to 20 rad/sec in the transfer function. This increases the frequency control region. Omission of motor M_1 provides faster response.

Consider Fig. 16 The outputs of the phase sensitive rectifiers are $K_1 \left[\cos \phi_i + \cos (2\,\omega_c t + \phi_i)\right]$

and $K_1 \left[\sin \phi_i + \sin (2\,\omega_c t + \phi_i)\right]$ respectively.

The transfer function of the networks Y_1 and Y_2 are of the form

$$Y_n = \frac{S + \frac{1}{\tau_n}}{S + \frac{1}{a\tau_n}} .$$

τ_1, τ_2 and a are chosen so that for frequencies up to approximately 4 rad/sec the output of Y_1 is approximately of the form $\phi_i + \tau_1 (1-a) \frac{d\phi_i}{dt}$ and that of Y_2 $\frac{a}{2}$. These outputs are fed into the balanced modulator and used as an error signal to correct the phase and frequency error of the drum. For frequencies between 4 rad/sec and 20 rad/sec the output

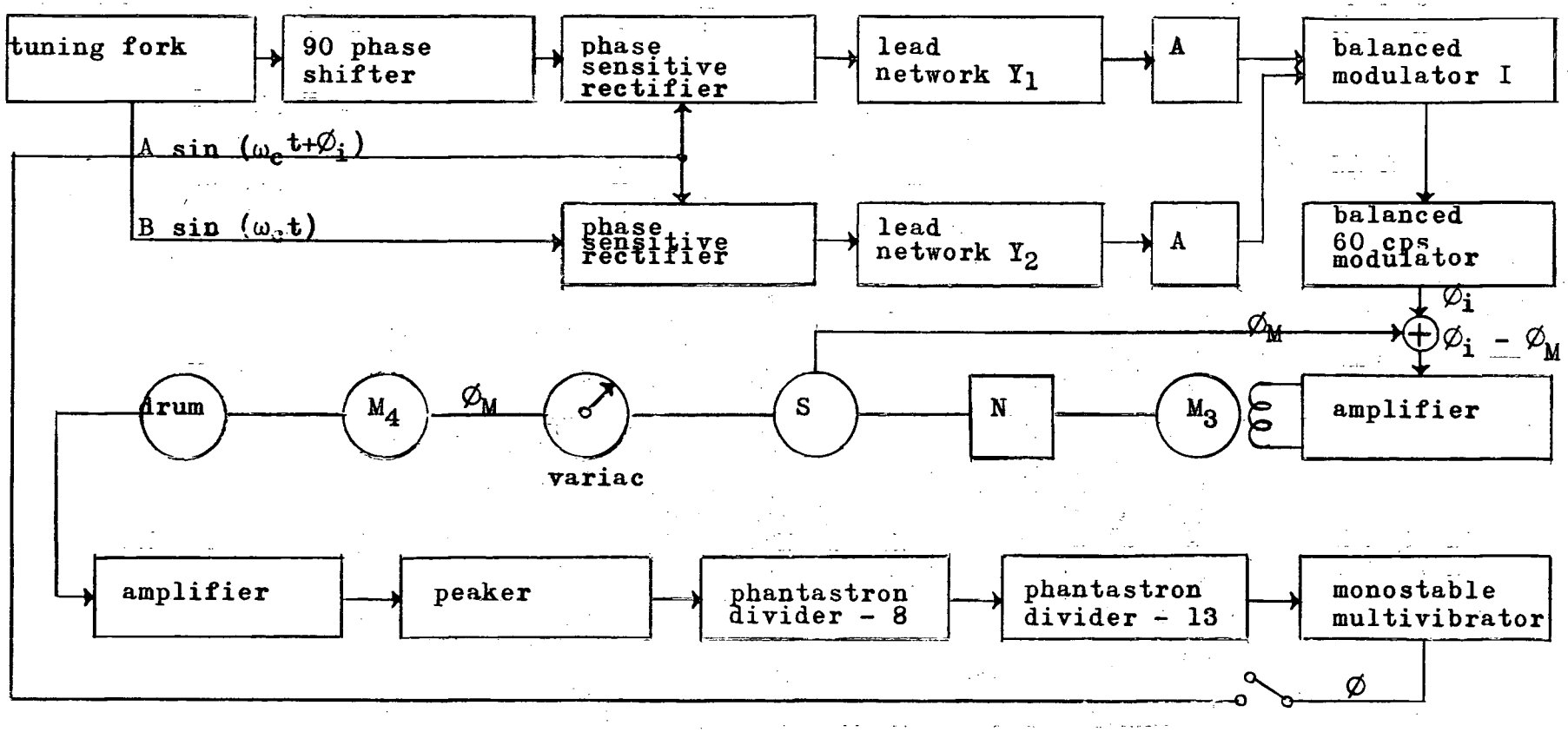

Figure 16. Block Diagram of Revised Design

of the balanced modulator will be mainly determined by a term of the form $\frac{(1-a)}{2} \quad \frac{d\phi_i}{dt}$.

This means that for low frequency changes phase and frequency control is provided, for high frequency changes frequency control is provided.

The high frequency component $(2\,\omega_c t + \phi_i)$ is greatly attenuated in the phase sensitive rectifier.

Let

k_3 and k_4 be coefficients of proportionality referring to motor M_3 and M_4 respectively

k_s the synchro displacement in volts/rad

G_1 the DC gain of the phase sensitive rectifier in volts/rad

G_2 the gain of the DC amplifier

G_3 the gain of the modulators.

Fig. 17 shows the lead networks Y_1 and Y_2.

The transfer function is of the form $a \; \frac{1 + S\tau_n}{1 + as\tau_n}$.

For Y_1 $a = 1/10$ and $\tau_1 = 2.2$ rad/sec and

for Y_2 $a = 1/10$ and $\tau_2 = 0.5$ rad/sec

where $a = \frac{r_o}{r + r_o}$ and $T = r\,C$.

Assume the loop to be open (see Fig.16) and the output of the drum to be ϕ. The transfer function of the drum and motor M_4 is

$$\frac{\phi}{\phi_M} = \frac{k_4}{S(S + \frac{1}{\tau_4})}$$

and that of the amplifier and motor M_3

$$k_3(\phi_i - \phi_M)\, A = J_3 S(S + \frac{1}{\tau_3})\, \phi_M \quad ,$$

$$\frac{\phi_M}{\phi_i} = \frac{1}{1 + \frac{J_3}{k_3 A}\; S(S + \frac{1}{\tau_3})} \quad .$$

Therefore the open loop over-all transfer function is

$$\frac{\phi}{\phi_i} = \frac{(G_1\, G_2\, G_3\, k_4\, k_s)\, (S + \frac{1}{\tau_n})}{S(S + \frac{1}{\tau_4})\, (S + \frac{1}{a\tau_n})\quad 1 + \frac{J_4}{k_3 A}\; S(S + \frac{1}{\tau_3})} \quad .$$

The Nyquist plot of the transfer function has the general shape as Fig. 14a. The constant should be chosen so that the loop is stable. The maximum value of the constant has to be determined experimentally. For $\tau_n = \tau_1$ the constant $(G_1\, G_2\, G_3\, k_4\, k_s)$ should be approximately 28 in order to provide an overshoot of not more than 3.0 db at the high frequency end of the closed loop transfer function (see Fig.18 and 19).

Fig. 17 shows a detailed circuit diagram of the phase sensitive rectifiers, lead networks, amplifiers, and balanced modulators. The outputs of the phase sensitive rectifiers are transmitted in push-pull to the balanced modulators through the lead networks and the amplifiers. Due to the fact that $\frac{d}{dt} \cos \phi_i = -\frac{d\phi_i}{dt} \sin \phi_i$ the transfer function Y_2 must have the form

$$Y_2 = a\, \frac{1 - S\tau_2}{1 + aS\tau_2}$$

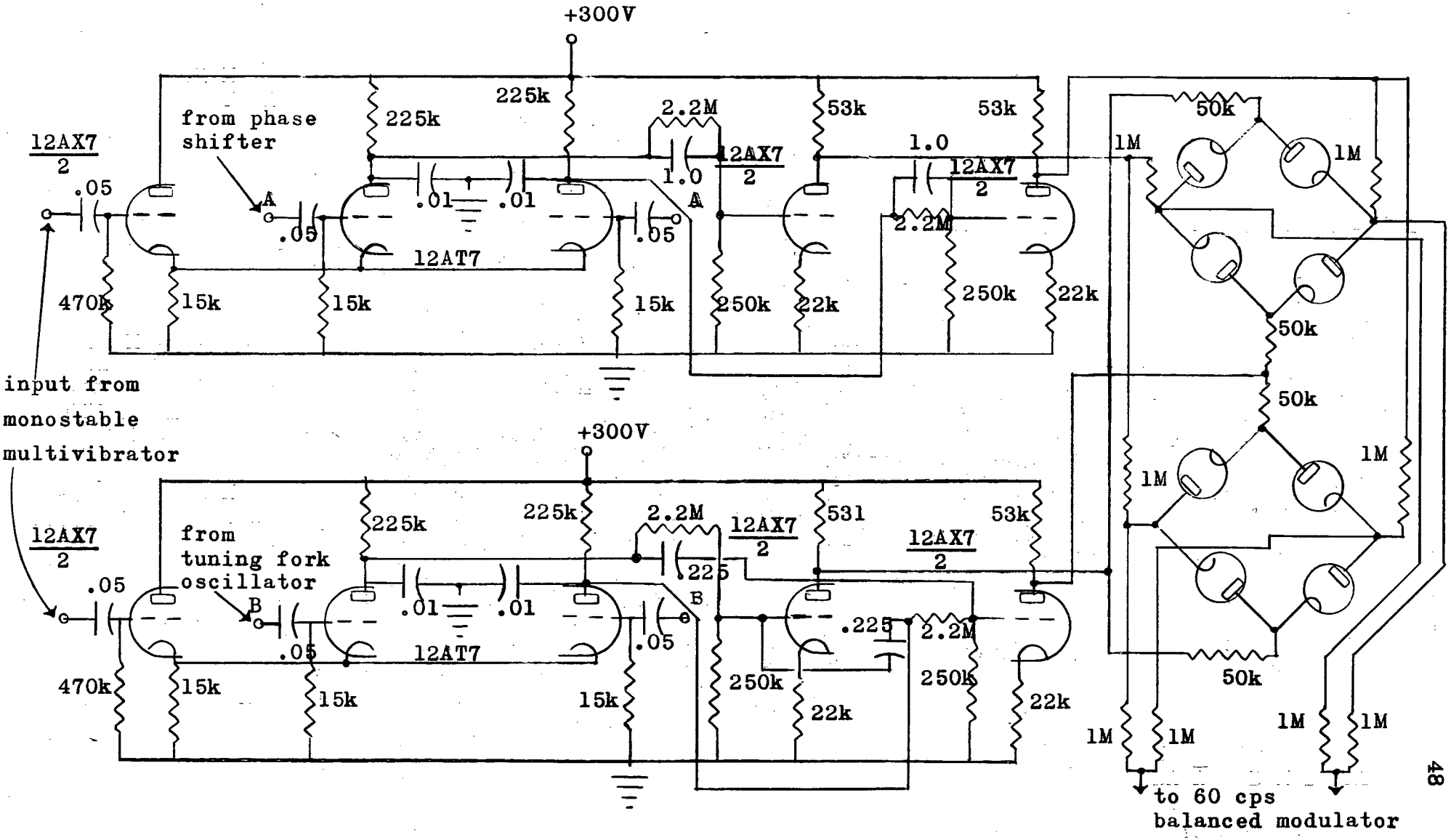

Figure 17. Phase Sensitive Rectifier, Leadnetwork, Amplifier, and Balanced Modulator

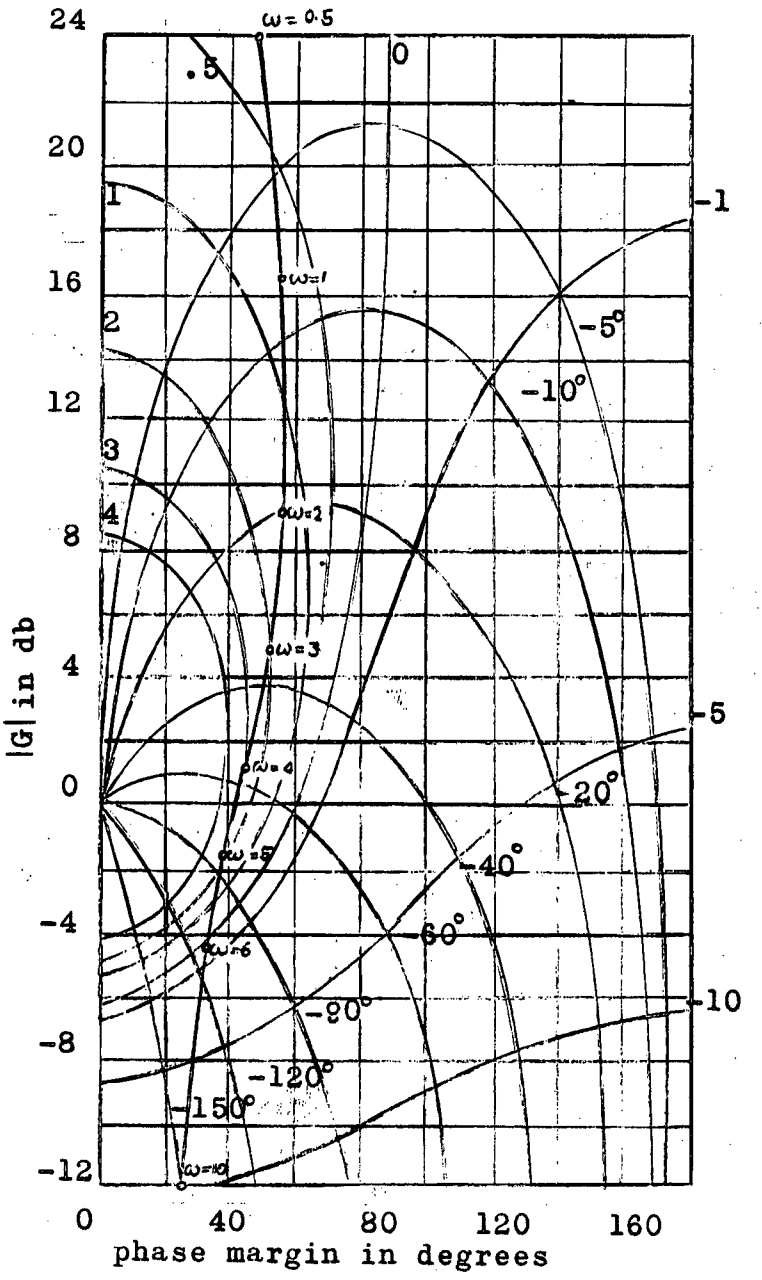

Figure 18. Open and Closed Loop Response of Revised Design

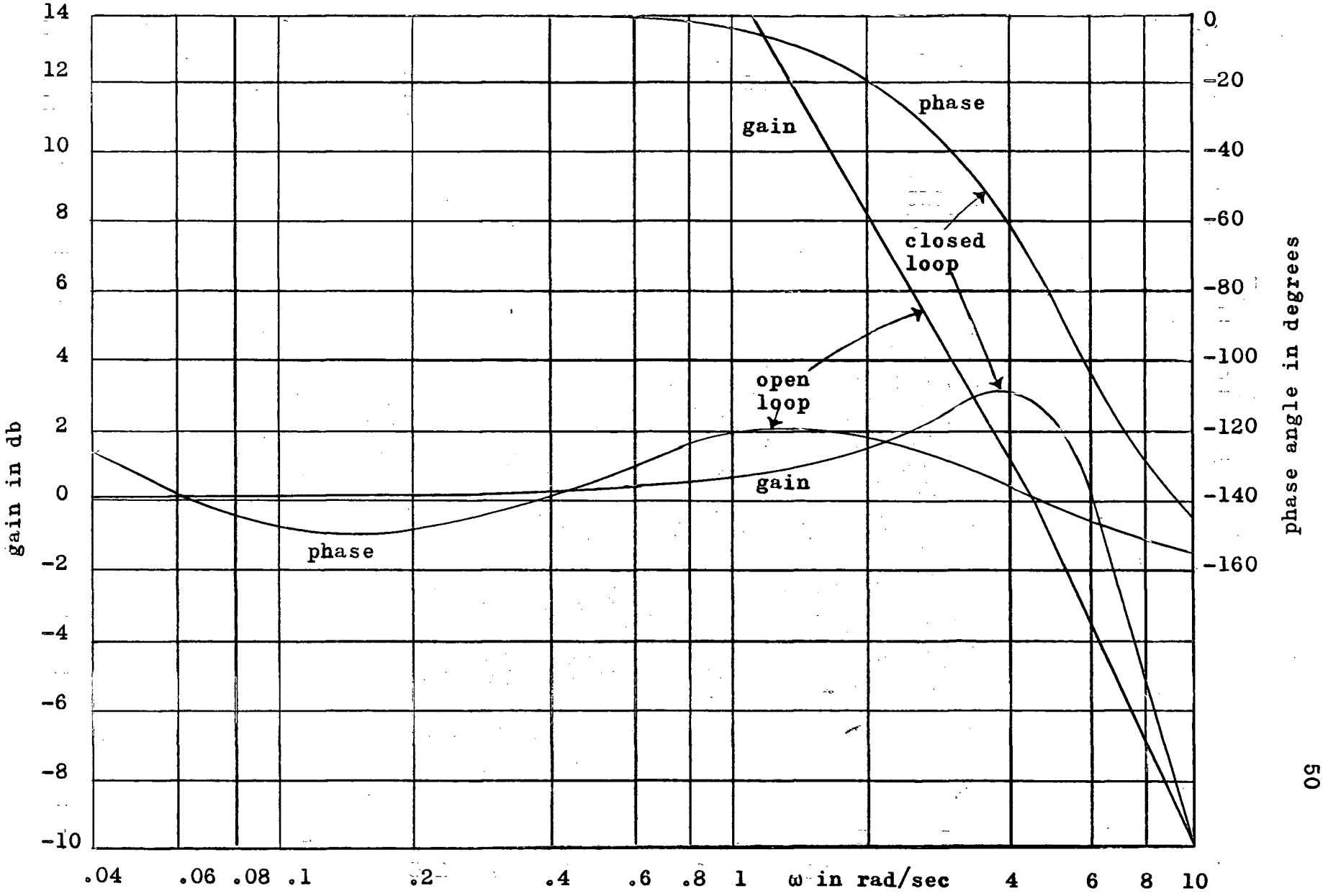

Figure 19. Open and Closed Loop Response

This can be achieved by crossing over the condensers in the lead network Y_2. Therefore the output of the balanced modulator for a signal frequency between 4 rad/sec and 20 rad/sec will be of the form $(\frac{1-a}{2} \quad \frac{d\phi_i}{dt})$.
The amplitude of this term drops with increasing frequency. At 10 cps there is still sufficient output to move the variac.

Consider Fig. 20. The output of the balanced modulator is fed by push-pull into a 60 cps modulator, the output of which is added to the synchro signal at the grid of the push-pull power amplifier. The output of the power amplifier is the error signal which drives the variac motor M_3.

For the motor M_3 there are two distinct modes of operation. For Mode I the phase angle ϕ_i is small so that $\sin \phi_i = \phi_i$ and M_3 operates as a phase detector. Its shaft rotation indicates the phase error and the variac movement is directly proportional to the phase error. The lead network Y_1 is used to stabilize this mode of operation.

For Mode II there is a frequency error. The lead network Y_1 has no longer any appreciable phase lead. However Y_2 functions as a lead network at higher frequencies. The DC output of the balanced modulator I is proportional to $\frac{d\phi_i}{dt}$. The servo M_3 filters out the fluctuating term due to changing phase. The shaft rotation is therefore proportional to the frequency error.

This revised system meets all the above requirements. The automatic mode switching feature inherent in the system

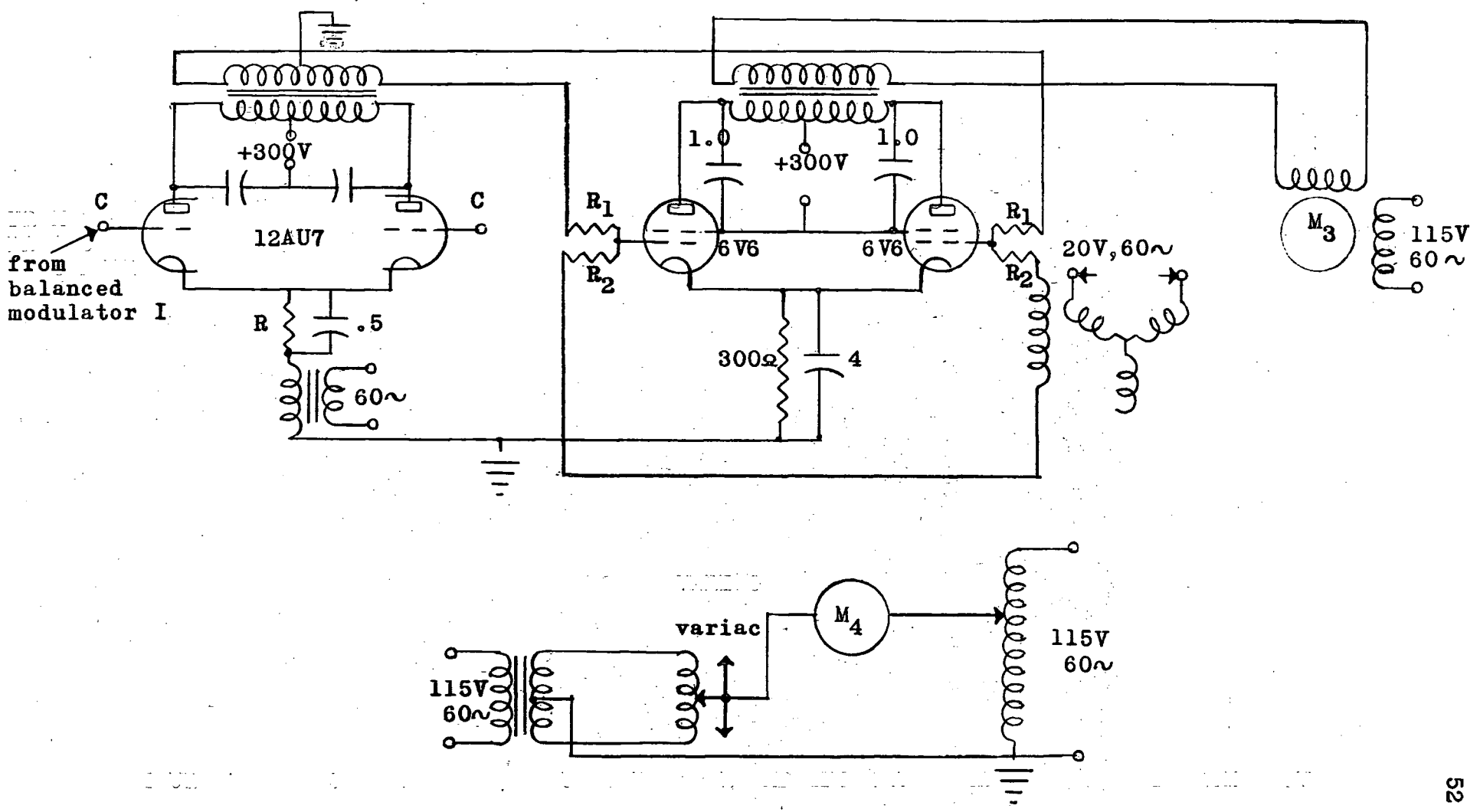

Figure 20. 60cps Balanced Modulator, Power Amplifier, and Bias Setting of Drum Drive Motor

gives an extended frequency control range and a stable phase control region. The signals are applied directly to the variac drive motor M_3 which improves the response. Time did not permit testing the revised system.

CHAPTER VI

The Precision Power Supply

Introduction

To satisfy the power supply requirements of the computer three separate units have been constructed. These consist of the following:

Power Supply #1. This is a precision ± 300 volts DC 450 mA unit with a voltage regulating tube for short term stability and a mercury cell for long term stability. This unit is to supply all the precision computing circuits.

Power Supply #II. This is similar to unit #1 with the exception that the mercury cell is not required. This unit is to supply all the pulse circuitry of the computer consisting of multivibrators, gates, dividers, etc.

Power Supply #III. This unit is the same as #II but supplies only + 300 volts DC and is used to supply the power for the output stages of all servoamplifiers.

Since the power supplies are nearly identical only unit #1 will be described here.

The power supplies were developed by modifying existing designs. (See reference 4, 5 and 8).

GENERAL DESCRIPTION

Fig. 21, 23, 24 and 25 show the two loops (a) and (b) that achieve the desired performance. With the modulator comparison circuit short-circuited, loop (a) gives approximately ± 300 volts. With the loop (b) in operation the sampling circuit is adjusted to give precisely ± 300

volts output.

Consider first the - 300 volt supply (Fig.21 and 23). The reference element (mercury cell) will detect any error due to drift of the -300 volts. This drift voltage is fed into the modulator comparison circuit which consists of a 60 cycle DC-AC chopper, an AC amplifier and a DC filter. Any deviation in output as seen at the contacts of the chopper produces an AC signal representing the error in magnitude and phase. This error will finally correct loop (a). Loop (b) corrects only for relatively slow changes while loop (a) corrects for several thousand cycles per second, due to a V.R. tube as reference element. The output capacitor of the power supply reduces the impedance at high frequencies.

It is now possible to regulate the +300 volts using the regulated -300 volts and ground as fixed reference potentials. Loop (a) between ground and +300 volts is correcting again for high frequency changes. The error voltage is now obtained by comparing ground potential with a virtual ground on a voltage divider network between the +300 and the -300 volts. (Fig. 24 and 25).

Fig. 21 shows the power supply between ground and -300 volts, Fig. 22 the DC comparison circuit and amplifier, and Fig. 23 the modulator comparison circuit. At first the section between -300 volts and ground should be calibrated.

Fig. 24 shows the section of the power supply between ground and +300 volts, and Fig. 25, the modulator

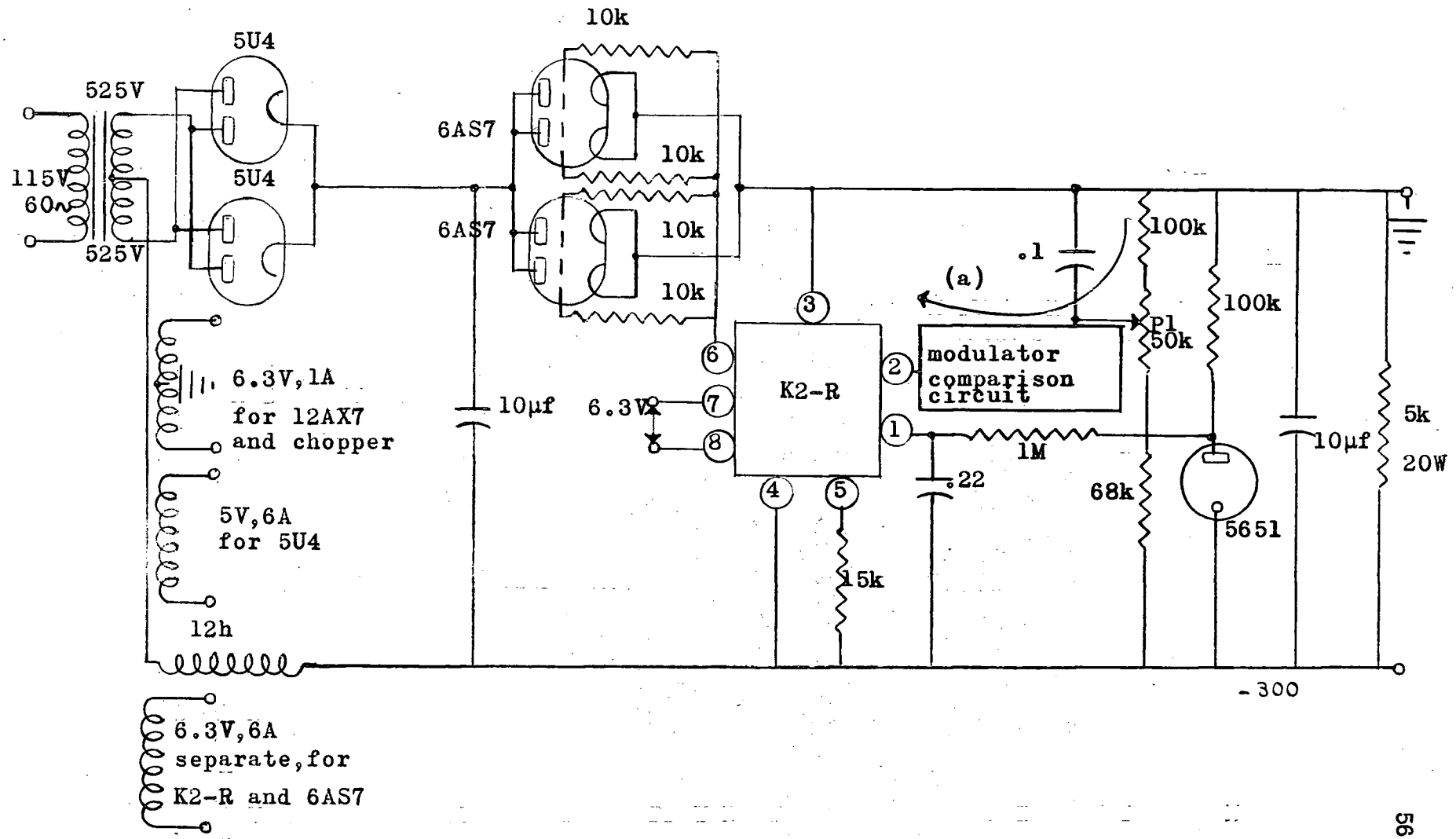

Figure 21. Precision Power Supply between -300 V DC and Ground, 450 mA

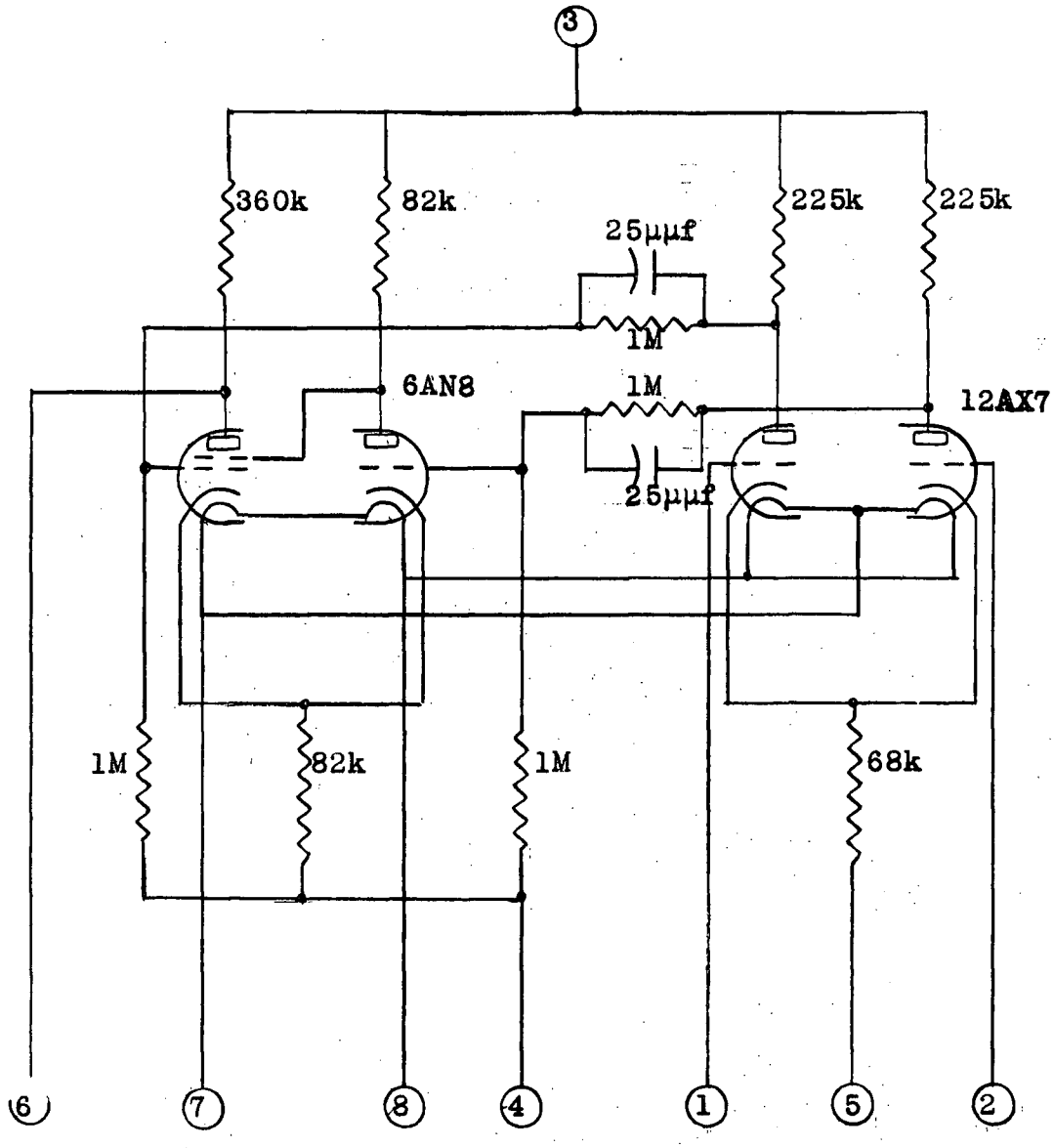

Figure 22. DC Comparison Circuit and Amplifier, George A. Philbrick, Model K2-R

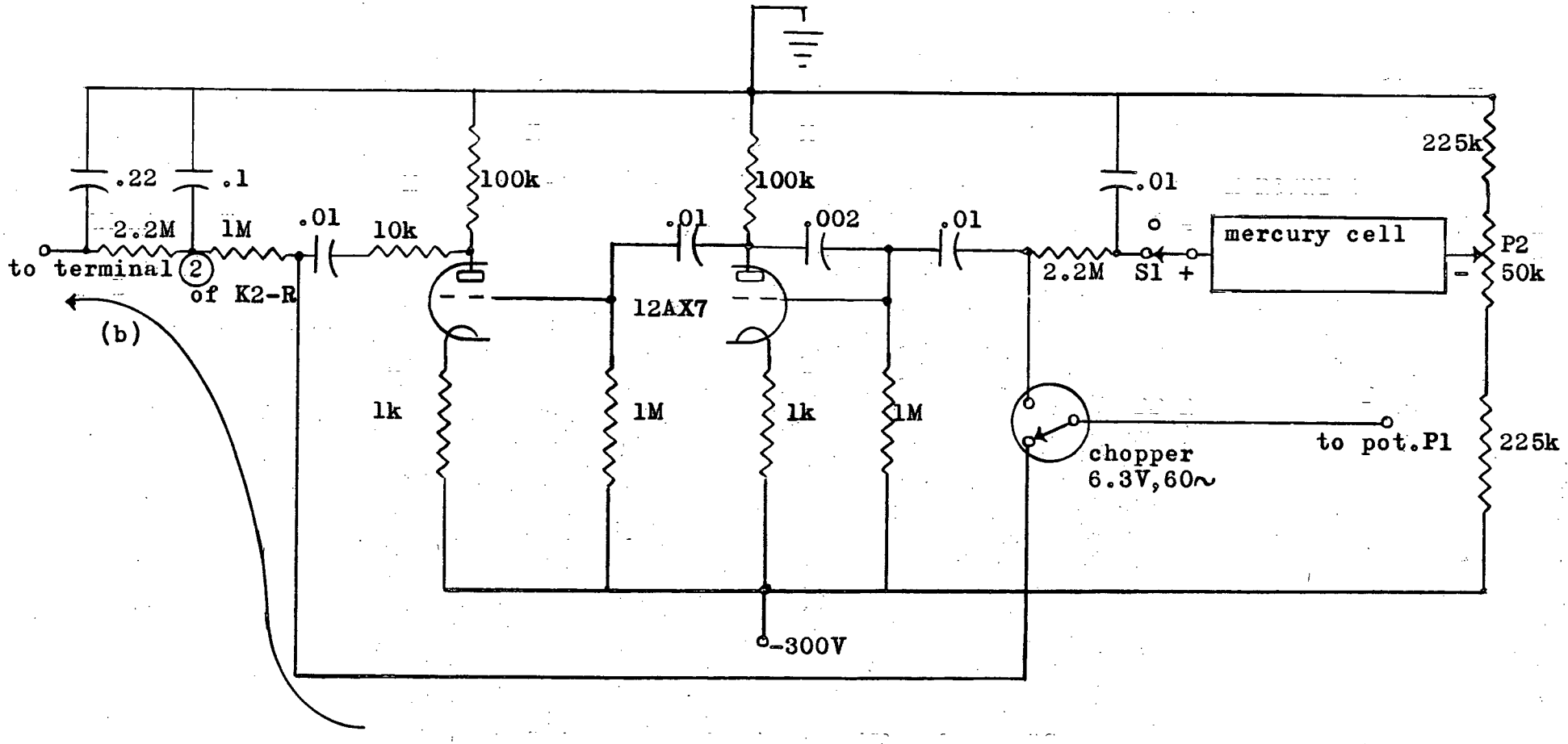

Figure 23. Modulator Comparison Circuit

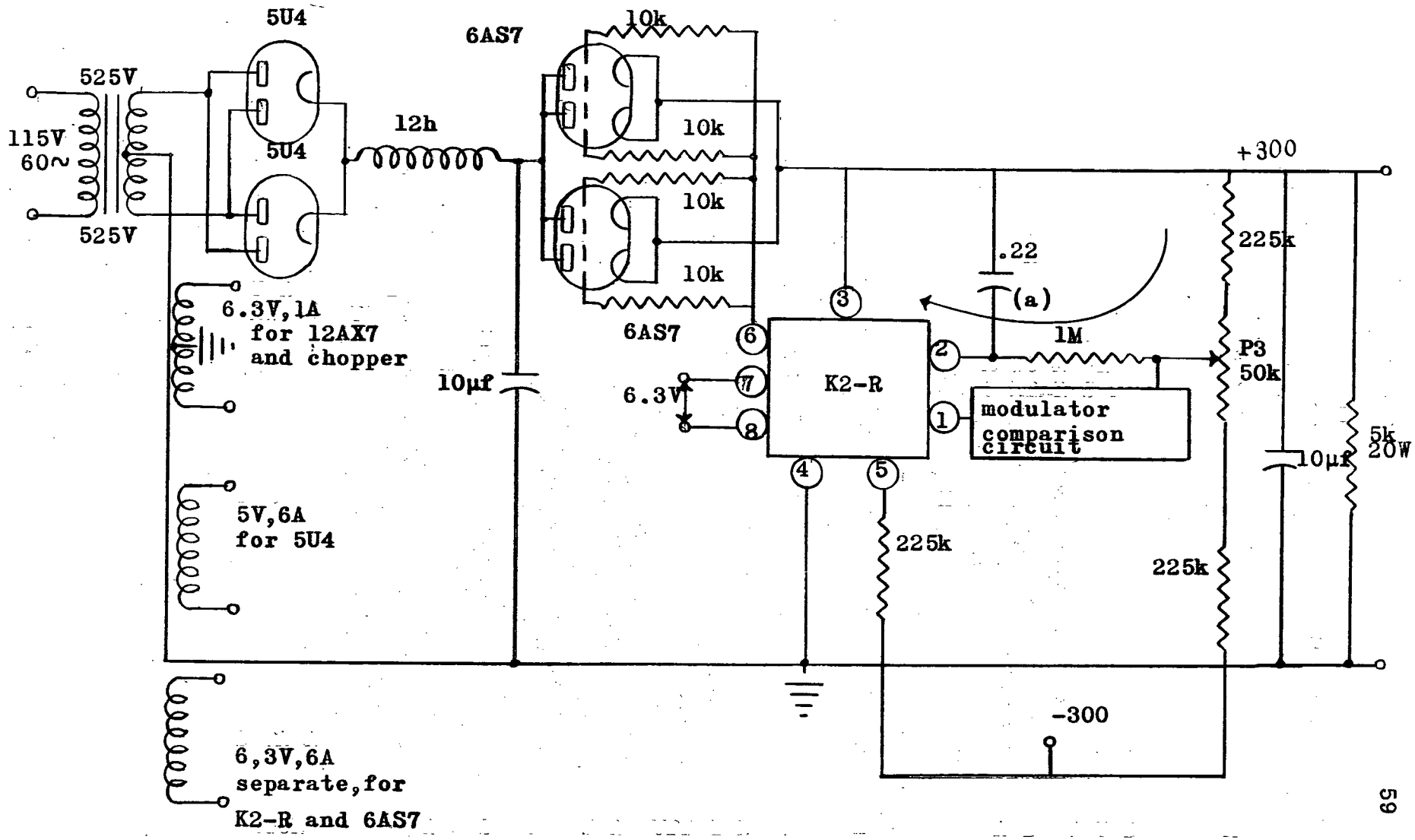

Figure 24. Precision Power Supply between +300 V DC and Ground, 450 mA

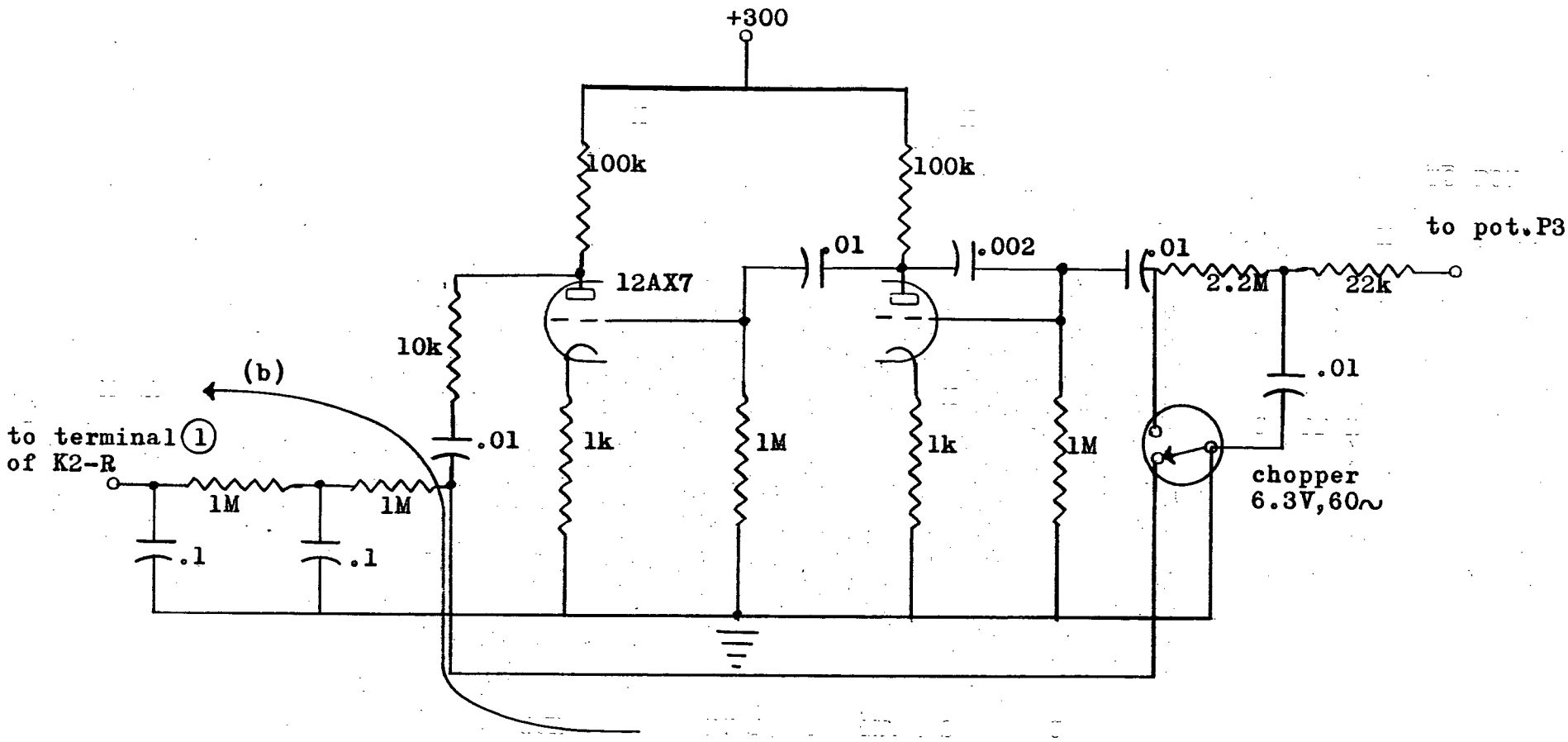

Figure 25. Modulator Comparison Circuit

comparison circuit. The section between ground and +300 volts should be calibrated after the section between -300 volts and ground has been calibrated.

Calibration Procedure

1. Open switch S1.
2. Adjust potentiometer P1 so that the output is - 300 volts DC.
3. Close S1.
4. Adjust P2 so that output is again -300 volts DC.
5. Adjust P3 so that output is +300 volts DC.

References

1. Ahrendt, W. R., Servomechanism Practice, New York, Toronto, London, McGraw-Hill 1954.

2. Brown, Campbell, Principles of Servomechanism, John Wiley and Sons Ltd., New York 1948.

3. Chance, Hughes, MacNichol, Sayre and Williams, Waveforms, McGraw-Hill, New York, Toronto London, M.I.T.Radiation Laboratory Series vol.19.

4. Ernst, W. P., Stable Power Supply for Microwave Standards, Electronics, 27, Page 168 January 1954.

5. Greenwood, Holdam and MacRae, Electronic Instruments, New York, Toronto, London, McGraw-Hill,1948 M.I.T. Radiation Laboratory Series vol.21.

6. James, Nichols, Phillips, Theory of Servomechanism, New York, Toronto, London, McGraw-Hill 1948. M.I.T. Radiation Laboratory Series, vol. 25.

7. Martin, Th. L. Jr., Electronic Circuits, New York, Prentice-Hale, Inc. 1955.

8. G.A.Philbrick Research Inc., Boston 10, Mass. Regulated Power Supply, GAP/R Model RK and GAP/P Model K2-R .

9. Seely, J., Electron-Tube Circuits, New York, Toronto, London, McGraw-Hill, 1950.

10. Valley, Wallman, Vacuum Tube Amplifiers, New York, Toronto, London, McGraw-Hill, 1948, M.I.T. Radiation Laboratory Series, vol.18.

11. Williams and West, The Position Synchronization of a Rotating Drum, Proceedings of the I.E.E., vol. 98, 1951, p.30.

APPENDIX

List of Components

DC-AC Chopper	Type 344, Coil 6 volts, manufactured by Stevens and Arnold, South Boston, Mass.
M_1 - T	MOTOR GENERATOR SET 880100 6.5 Watt, Manufactured by Sangamo 115V per phase, 60 cycles, 3350 RPM tachometer of fixed frequency type with output of 6.5 volts/1000 RPM.
M_2	Type FP-25-3. Low inertia servo motor, Diehl Manufacturing Company, 20 volts per phase, speed 3200 RPM. Current per phase 0.50 amps, 60 cycles.
M_3	Type M623. Brown Balancing Motor, Minneapolis-Honeywell, gear reduced two phase, low inertia 115 volts, 13.5 watts, 27 RPM 60 cycles.
N_1	Gear reduction 27:1.
N_2	666: 1 reduction.
N_3	Included in N_3 approximately 32:1.(Original design).
Output Transformer	For 60 cycles, adjustable loads.
Resolver	Type FJE-43-9, Manufactured by Diehl, designed for 400 cycles at 115 volts.
Magnetic Storage Drum	Magnetic Storage Drum, manufactured by Librascope, Serial No. 1, Model No. 179-3. Motor data: 115 volts, 60 cycles, 10,000 RPM 1/10 H.P.

S_1 and S_2	Type 403-02. Synchro receiver and synchro transmitter. Manufactured by Kollman for 60 cycles operation. Accurate to within .75 degrees.
Tuning Fork	General Radio Corporation, type 723, vacuum-tube fork 1000 cycles $\pm$ o.o5%.
Variac	Type 200B, General Radio Company, Bainbridge, Mass., U. S. A.